NTNU – Trondheim
Norwegian University of
Science and Technology

Size Distribution for Oil Droplets Dispersed in Water

An Experimental Study by Image Analysis

Erling B Grammeltvedt

Petroleum Geoscience and Engineering
Submission date: June 2014
Supervisor: Harald Arne Asheim, IPT

Norwegian University of Science and Technology
Department of Petroleum Engineering and Applied Geophysics

Summary

The work in this thesis is based on image analysis of oil droplets dispersed in water. It uses a public domain image processing program called ImageJ to analyse distribution of oil droplets generated by a breaking wave in a flume and by injecting trough a nozzle in a tank. The droplet distribution will evolve with time, due to buoyant forces in the water. One goal for the work was to get quantitative knowledge on how the distribution evolves and compare these to the expected values for the rising speed. Large droplets is expected to rise faster than small ones, and as a result the droplets will be sorted with time. A second goal was to compare the volume of droplets dispersed through a nozzle to predictions based on existing theory.

Some challenges were encountered while developing the design for the tank experiments. The use of a globe valve failed to disperse the oil into droplets. Only by use of direct injection through a nozzle was a distribution of droplets generated. One issue experienced was the resolution of the images used for image analysis. Focus and lighting used in the experiments affected the results, as the functions used to process the images gave large errors when analysing small droplets. For dense droplet distributions the image analysis failed completely because it could not separate droplets from each other. The values found in the tank experiments for droplet volumes and rising speed deviated considerably from the expected values. Together with errors from the handling of the images the oil viscosity and inter facial tension with water could have considerable effect on the droplets. For tests in the wave flume the suggestions made by Grammeltvedt (2013) worked with regards to lighting, but further improvements regarding sideways motion should also be handled.

Sammendrag

Arbeidet i denne masteroppgaven er basert på bildeanalyse av en fordeling med oljedråper spredt i vann. Til bruk i analysen av bildene er det benyttet gratis programvare kalt ImageJ. Dette programmet behandler bildene og analyserer dråpene som blir funnet. Eksperimenter ble gjennomført i en bølgekanal og i en vanntank. På grunn av oppdriften i vannet er det ventet at fordelingen over tid vil avta i gjennomsnittsverdi, samt gå mot mindre spredning i verdier. Et av målene for denne oppgaven var å sammenligne utviklingen av dråpeskyen og sotreringen av dråpene med forvetet stigehastighet. Videre ble det forsøkt å sammeligne dråpefordelingen, som et resultat av injeksjon gjennom en dyse, med teori anngående energi dispergeringen.

Under arbeid med å bygge anlegg for testing i tanken ble det brukt en ventil. Denne ga desverre ikke ønsket resultat hva angikk spredning av oljen. Derfor måtte det lages en dyse som injiserte olje rett inn i tanken. Analysen av bildene ga store feilkilder når det gjaldt størrelse for små dråper. Grunnet oppløsning og fokusering i bildene var det vanskelig å anslå noe klar grense for utstrekningen til dråpene. Dette satte enkelte begrensninger for hvor små dråper som kunne identifiseres. Videre var det vanskelig å gjøre beregninger på dråpefordelinger der dråpene sto tett eller overlappet hverandre fordi de automatiske funkjsonene i bildebehandlingsprogrammet her ikke klarte å skille dråper fra hverandre. Resultatene fra forsøk gjort i vanntanken ga store avvik fra det som var forventet fra teorien. Noe av dette skylles trolig viskositeten til matoljen som ble brukt og overflatespenningen mellom oljen og vannet. Når det gjelder forsøkene i bølgekanalen viste disse at det var gode betingelser med tanke på endringer som ble gjort i belysningsoppsettet sammenlignet med Grammeltvedt (2013). Mye sideveis bevegelse i kanalen bør likevel utbedres dersom man vil generere enda mer konsistente data.

Acknowledgments

I would like to thank my supervisor Harald Arne Asheim for help and guidance with conducting the experiments. Thanks also for valuable input and discussions regarding theory, design and results.

Thanks also to Håkon Myhren and Terje Bjerkan working in the work shop at IPT, for help with manufacturing parts needed for my experiments.

Finally thanks to phd. student Katherine Rose Aurand for help with measuring of oil properties in the lab.

E.G.

Contents

List of Figures

List of Tables

Chapter 1

Introduction

In order to ensure effective oil spill response, quantitative knowledge of how oil acts on the sea surface is necessary. Breaking waves will mix floating oil down into the water. The oil will be present as droplets of varying size. Droplet size and distribution will determine how the fast droplets will rise back to the surface. Delvigne et al. (1988) (1993) experimented with dispersion of oil in a flume with breaking waves. Reed et al. (2009) extended the work and made use of images to analyse their results. Asheim and Sivertsen (2012) built and tested a similar flume which could generate single breaking waves at repeatable conditions. They found that the height and speed of the wave worked within non-linear theory for the flume. Asheim and Zsolt (2012) conducted several tests in the flume and found that measuring single droplets in a dispersed distribution was possible by image analysis. They did introductory analysis on images with the purpose of communicating the visual impression of how the droplets are dispersed by breaking waves. They also concluded that a log-normal approach for droplet size distribution was adequate to describe the droplets based on only two parameters. Further analysis of their images was done by Grammeltvedt (2013). He found that issues regarding lighting and motion in the image series complicated the analysis. In order to expand the sample size and enhance repeatability some improvements was suggested. This thesis covers the work done to improve on these conditions. A different set up for the lighting was developed for experiments in the wave flume. In addition a standing tank was built to study the development of a droplet distribution at static water conditions. The goal was to link the energy dissipation to the droplet distribution and to compare the development with time to the theoretical rising speed for the droplets.

Chapter 2

Preliminary Studies

2.1 Dispersion of oil in water

Dispersion of surface oil by breaking waves

Understanding how a layer of surface oil is dispersed and entrained by breaking waves is mostly based on work by Delvigne and Sweeny (1988) and further described by Delvigne (1993). They experimented with dispersion of oil by breaking waves in two different flumes

- Medium sized flume. Length: 15 m, width: 0.5 m and depth: 0.43 m.
- Large flume. Length: 200 m, width: 5 m and depth: 4.3 m.

and supported their numerical data with results from a tank with an oscillating grid to create stable conditions. Both the flumes were equipped with a wave generator which created a train of breaking waves in the test section. Samples of the droplet size distribution were taken by test tubes which were submerged in the water and then opened to acquire samples at desired locations. Their theory was that dispersion of oil could be linked directly to the energy dissipation. Energy dissipation for the breaking waves was in turn estimated based on average wave height and not linked directly to their experiments. They concluded that the entrainment of oil droplets was strongly based on time after passing of the breaking wave and so their empirical data for maximum droplet size and droplet size distributions were based on steady state conditions. They suggested that maximum droplet size after a breaking wave was independent of

break-up process due to turbulence and rather dependent on resurfacing parameters, such as intrusion depth and rise velocity in addition to a vertical diffusion coefficient. Dunnewind et al. (2003) suggested a model for droplet size based on the turbulence and surface tension acting on the droplets. But their prediction has not been verified. Reed et al. (2009) attempted to extend the work of Delvigne et al. (1988,1993) into higher viscosity, non-Newtonian regions. They used a set up with a horizontal flume and a wave creator at the end. In addition they used image analysis for droplets with a diameter of 0.1 mm and upwards. Asheim (2011) introduced study of single breaking waves rather than wave trains. This was done in order to get controllable waves and to be able to quantify the energy dissipation. They used a relation between the dimensionless wave hight called a Froude number to express the dispersion force for a wave. Asheim and Sivertsen (2012) concluded that the energy dissipation could not be measured directly. The energy dissipation is related to a transition from mechanical to thermal energy, but the increase in temperature was almost too small to recognize with additional factors influencing it. Asheim and Zsolt (2012) used image analysis to describe the distribution of optically visible oil droplets created by a single breaking wave. They found that distributions with a large amount of droplets could be easily described by the log-normal distribution.

Dispersion of oil injected through a nozzle

Asheim (2012) made an attempt to predict droplet sizes based of the pressure loss across a valve based on the fundamental principles defined by Hinze (1955). According to Hinze maximum droplet size can be estimated from

$$d^* = 0,725 \frac{1}{\epsilon^{\frac{2}{5}}} \left(\frac{\sigma}{\rho}\right)^{\frac{3}{5}} \tag{2.1}$$

where σ is the surface tension and ρ is the oil density. The ϵ term can be defined as added energy per unit mass and time and expressed as

$$\epsilon = \frac{\Delta p Q}{m} \tag{2.2}$$

However the unit mass m is not well defined. It must represent the mass in the area the energy

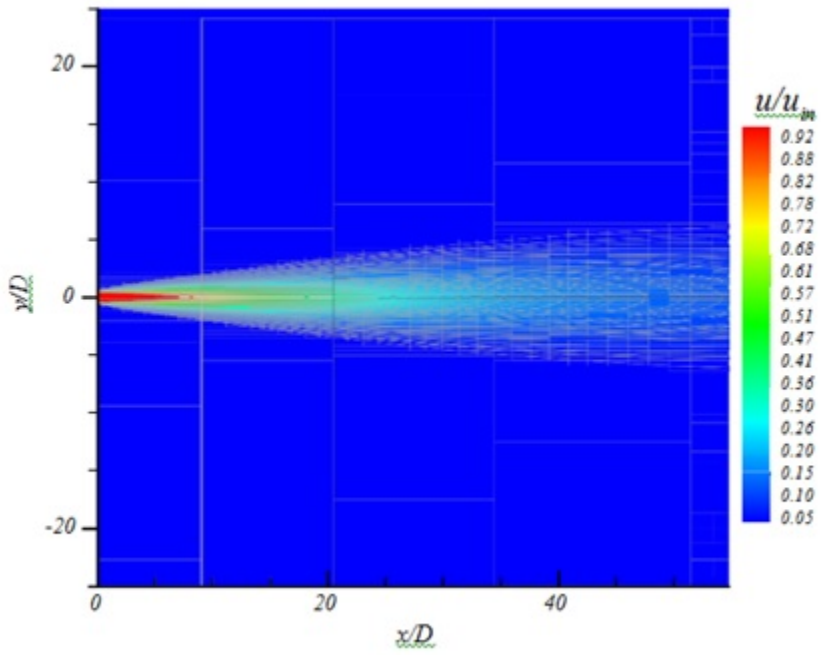

Figure 2.1: Visualization of jet stream (Asheim, 2012)

is dissipated. Previous studies has connected this to the pipe diameter to which the valve is connected. If however the valve is connected to a tank this assumption is not valid. If we still follow in the same way of thinking the unit mass or equivalent unit volume, V_d can be connected to the spreading of a free jet-stream. Example of a jet-stream can be seen in figure 2.1. If we seek the area where the dissipation is of the greatest magnitude, it should be possible to link this to the dimensionless length and with:

$$V_d \equiv \frac{V}{D^3} = \left(\frac{y}{D}\right)^2 \frac{x}{D} \tag{2.3}$$

The unit mass is then given by

$$m = \rho V = V_d \rho D^3 \tag{2.4}$$

and the energy dissipation can be expressed as

$$\epsilon = \frac{\Delta pQ}{m} = \frac{\pi}{4} \frac{\Delta p v}{V_d \rho D} \tag{2.5}$$

The velocity for a given pressure loss can be expressed:

$$v = \sqrt{\frac{2\Delta p}{\rho}} \tag{2.6}$$

Finally the rising speed for a spherical droplet with density ρ_o, rising in water with viscosity μ and density ρ_2 can, according to Stoke be expressed as:

$$v = \frac{gd^2}{18\mu}(\rho_w - \rho_o) \tag{2.7}$$

2.2 Rise velocity of a single droplet

Small droplets

Small droplets of oil are considered to be spherically shaped (Asheim and Zsolt, 2012). Rising velocity for a single droplet can be calculated from basic forces acting on it. Both buoyant and gravitational forces work on the droplet proportional with the volume (V_d) of the droplet. The sum of these forces can be expressed as

$$F_b = (\rho_w - \rho_o) g V_d \tag{2.8}$$

where ρ_o and ρ_W is the oil and water density respectively. Drag force will work in opposite direction of the movement. The force is considered proportional to the friction factor (f_d), the cross-sectional area of the droplet (A_d) and the rising velocity of the droplet (v_d) squared

$$F_d = \frac{1}{2} f_d \rho_w v_d^2 A_d \tag{2.9}$$

For a droplet travelling with constant speed the buoyant and drag forces are equal. The rising velocity is proportional with the square root of the droplet diameter (d) expressed as

$$v_d = \sqrt{\frac{4}{3}\frac{gd}{f_d}}\sqrt{\frac{\rho_o - \rho_w}{\rho_w}} \tag{2.10}$$

The friction factor is dependent on the Reynolds number (Re) of the interface between oil and

water

$$Re = \frac{\rho v_d d}{\mu} \tag{2.11}$$

which in turn is inversely proportional to the viscosity (μ) of the surrounding water.

Larger droplets

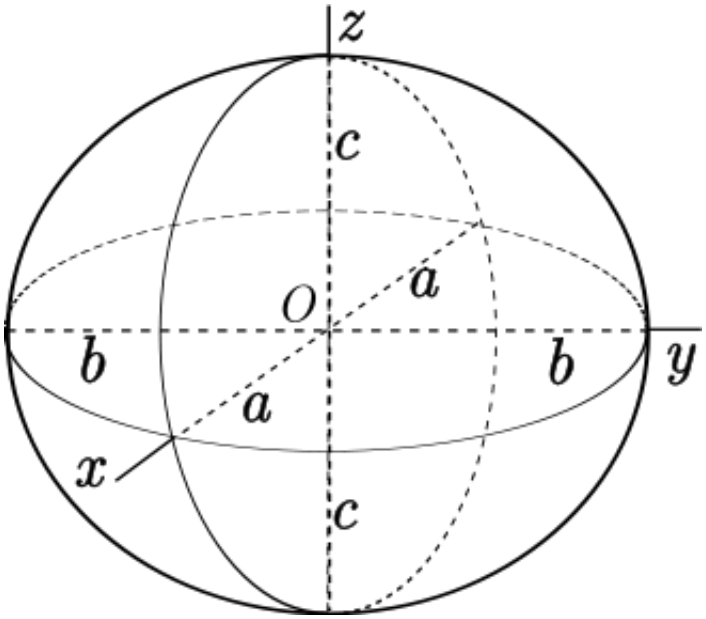

Figure 2.2: Ellipsoid with distinct semi-axes a, b and c (Mercator, 2012)

Larger droplets will deviate from small ones in shape because of density and flow. Density difference between oil and water makes the droplets slightly flattened (Asheim and Zsolt, 2012). Ellipsoids (figure 2.2) seem to be a reasonable approximation. We assume symmetry about the z axis. The volume of the droplet can be estimated based on the largest and smallest values of the cross section of the droplet. These cross sections are referred to as Feret diameters, for the shortest half axis $c = \frac{d_{min}}{2}$ and for the longest half axis $a = b = \frac{d_{max}}{2}$. The volume of the droplet can be expressed as

$$V = \frac{4}{3}\pi \frac{d_{min}}{2} \left[\frac{d_{max}}{2}\right]^2 \tag{2.12}$$

If we assume constant density and droplet shape, the rising speed could be derived in the same way as for spherical droplets. However this may not be reasonable because of the previously mentioned mechanics of the droplet. Zheng and Yapa (2000) computed rising speed for larger

and non-spherical droplets.

2.3 Rise velocity for a droplet distribution

Rise velocity for the largest droplet

For a distribution of droplets rising together single droplets will change constantly. Turbulent forces will brake apart droplets while surface tension(σ) will keep them together (Dunnewind et al., 2003). For a droplet with surface area S_d the surface tension will contribute with a force $F_\sigma = \sigma S_d$. Turbulent forces can be considered proportional with the friction force from equation 2.9. Asheim (2013) found it reasonable to consider droplet size with regards to the forces acting on it. The Weber number (*We*) for a droplet can be expressed as

$$We = \frac{\rho_d v_d^2 d}{\sigma} \tag{2.13}$$

A critical Weber number can be found for different oil-water mixtures. This critical number is defined as the largest number for which a droplet can exist, while larger numbers will result in the droplet breaking apart. For the largest droplet in a cloud of droplets the rising velocity can be found by combining equation 2.10 and 2.13

$$v_d{}^* = K_d \left[\frac{g\sigma(\rho_w - \rho_o)}{\rho_w^2} \right]^{0.25} \tag{2.14}$$

where K_d are the dimensionless parameters

$$K_d = \left(\frac{4}{3} \frac{We^*}{f_d} \right)^{0.25} \tag{2.15}$$

The * star denotes values for the largest bubble in the distribution.

Flow dynamics for a distribution of droplets

The flow dynamics for droplets rising in a cloud will be quite different compared to droplets rising alone. Coherent droplets will merge with each other and turbulent forces will break big

Figure 2.3: Oil droplets rising in water, adapted from Asheim (2013)

droplets apart, illustrated in figure 2.3. This is a continuous process. Viscosity of the different fluids will affect the friction factor and the Weber number and temperature will affect interfacial tension. It also seems reasonable to expect a hindered rising effect similar to hindered settling for particles in stagnant fluid. The magnitude of this effect is given by the rheology of the surrounding fluid and the droplet dispersion. For some cases with rising oil plumes, the magnitude of droplets rising together in a cloud could be enough to locally lift the water level up for from static conditions into a dome shape. As the oil rises it will disperse and as a result remain distributed throughout the water column.

Chapter 3

Description

3.1 Wave flume

Design

The design of the flume was presented by Asheim (2011) while construction and testing were described by Asheim and Sivertsen (2012). The flume was designed to simulate the propagation and breaking of a single wave. This can be observed in the nature as "bores", tidal waves migrating up rivers. In this design the wave was generated mechanically pushing in one of the end-walls like a piston. This creates a waterfront which given enough speed will create a breaking wave. A schematic of the flume and the piston can be seen in figure 3.1 The speed of the

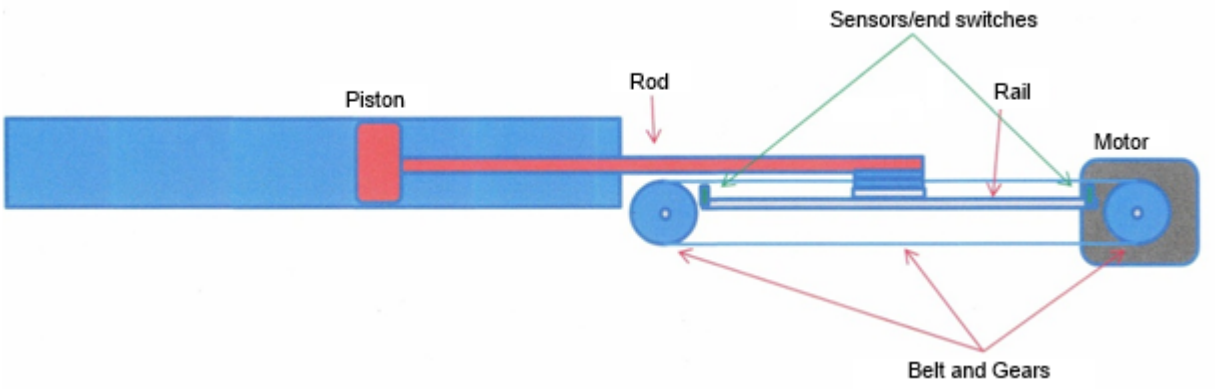

Figure 3.1: Schematic of flume with piston, adapted from Asheim and Sivertsen (2012)

Length	L =	10 m
Width	w =	0.3 m
Height	h =	0.3 m
Distance from piston to observation window	l_1 =	4.0 m
Distance from piston to observation window	l_2 =	6.0 m
Stroke length for the piston	l_s =	0.9 m

Table 3.1: Values for the wave flume

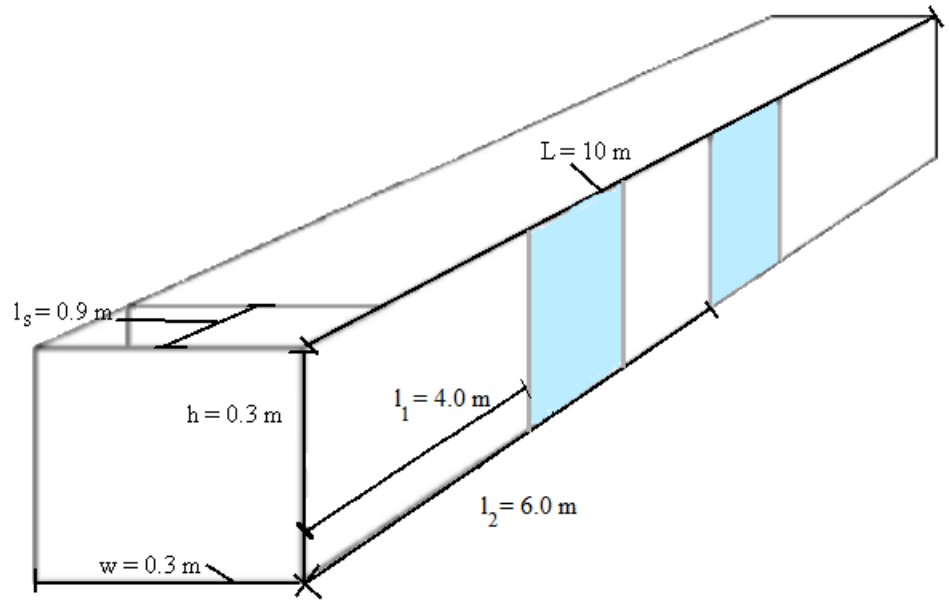

Figure 3.2: Drawing of the flume with dimensions

piston was controlled by adjusting the voltage of the electric motor. Asheim and Zsolt (2012) assumed the piston speed to be unaffected by the height of the water. The relations between wave height, Froude number and wave speed was derived by Asheim (2011). By controlling the height of the water and adjusting the speed of the piston the wanted speed, height and Froude number for the wave could be obtained. The dimensions of the flume can be seen in table 3.1 and figure 3.2.

Experiment conditions

Asheim and Zsolt (2012) conducted several different experiments were by altering the water level and piston speed. Each condition was tested multiple times. The parameters defining the different conditions are presented in table 3.2. They used soy oil with a measured density of 926 kg/m^3. The oil was coloured with sudan red in order to enhance the contrast between oil and water. Grammeltvedt (2013) analysed their images with focus on development of the droplet distribution. However several issues regarding lighting, sideways movement and length of image series gave few empirical and conclusive results. A new series of experiments in the wave flume was conducted to test some of the improvements suggested by Grammeltvedt (2013). The test conditions was kept similar to those of Asheim and Zsolt (2012) to generate the similar test conditions. However less oil was used, as the goal was to only create a small dispersion of droplets and investigations of oil concentration was not a goal. The oil used was also slightly different with regards to parameters. It was a vegetable oil with a measured density of 913,4 kg/m^3. Further the seals on the piston had swelled, so they had to be reworked. According to Asheim (2011) the flume was designed in such a way that the effect of the wall friction could be neglected. In addition a wave dampener was inserted. This wave dampener was designed as a sloped plate with a hight of 19 cm and an angle of 56°. It was placed 1.7 m from the end wall and had four holes beneath the static water level to allow the water which was forced over the top to flow back. Due to scratches in the glass on the observation window it was chosen to use another observation window closer to the middle of the flume. Assuming that all the parameters from Asheim and Sivertsen (2012) are valid the experiment conditions can be seen in table 3.3. One test run was conducted for each of test conditions seven and eight while three runs were conducted for test condition nine.

Wave description

Figure 3.3 shows an example image from the experiments. This image was taken from test condition one on the fourth run. It shows the oil floating on top of the water in the flume. The pencil line at the top is 200 mm long and used to set the scale for the image analysis.

Figure 3.4 shows the wave as it passes the observation window. Wave hight with reference to

	Voltage	Water level	Piston speed	Froude Number	Wave Speed	Wave Height
1	4.0 V	0.10 m	0.869 m/s	0.877	1.72 m/s	0.102 m
2	3.0 V	0.10 m	0.687 m/s	0.693	1.55 m/s	0.079 m
3	3.0 V	0.15 m	0.687 m/s	0.566	1.77 m/s	0.096 m
4	2.5 V	0.15 m	0.587 m/s	0.484	1.68 m/s	0.081 m
5	2.0 V	0.15 m	0.481 m/s	0.397	1.59 m/s	0.065 m
6	2.5 V	0.12 m	0.587 m/s	0.541	1.55 m/s	0.073 m

Table 3.2: Experiment parameters used by (Asheim and Zsolt, 2012)

	Voltage	Water level	Piston speed	Froude Number	Wave Speed	Wave Height
7	2.5 V	0.15 m	0.587 m/s	0.484	1.68 m/s	0.081 m
8	2.5 V	0.12 m	0.587 m/s	0.541	1.55 m/s	0.073 m
9	2.5 V	0.10 m	0.587 m/s	N/A	N/A	N/A

Table 3.3: Experiment parameters for tests with improved lighting, assuming valid values from Asheim and Sivertsen (2012)

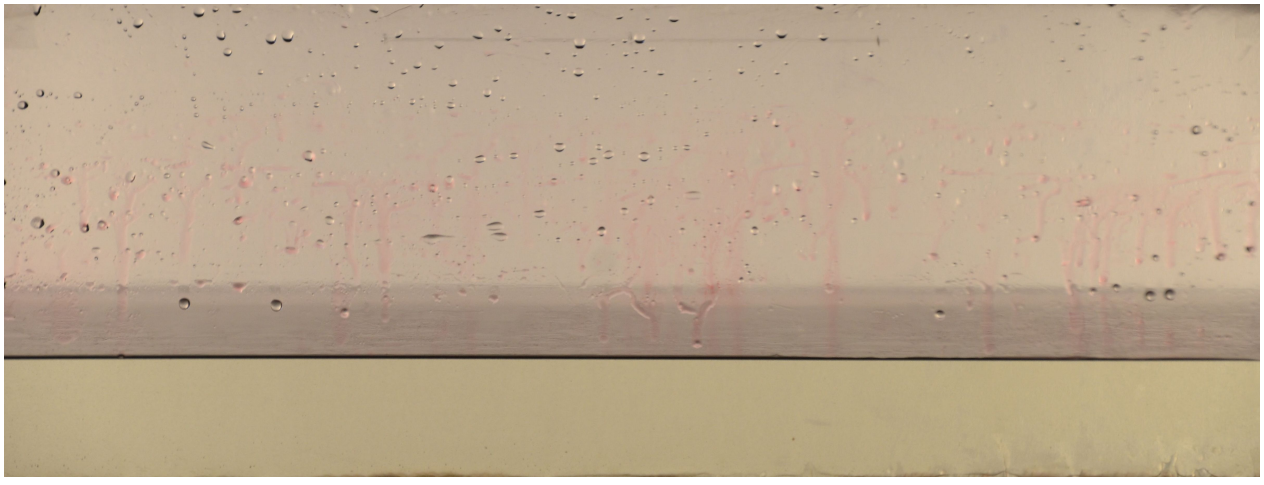

Figure 3.3: Image from test condition nine at static conditions

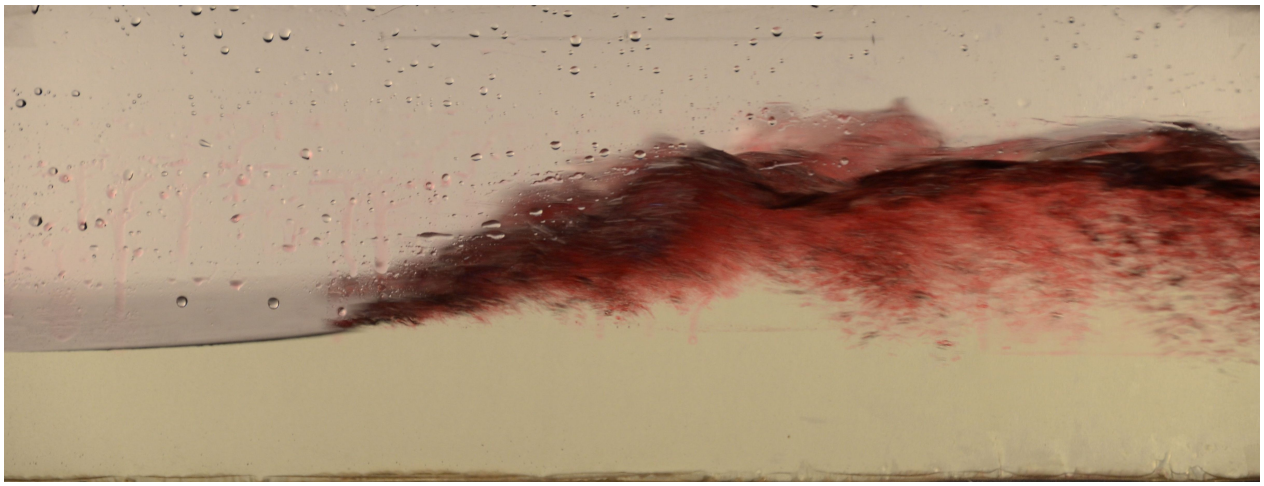

Figure 3.4: Image from test condition nine when the wave passes the observation window

the static hight can be compared to the water level in front of the wave. The wave drives the oil in front of it which results in high oil concentration at the front. At the back of the wave turbulence mixes oil droplets down into the water column. When the wave hit the wave dampener and the end wall it was returned. Whenever the wave passed the observation window a period with high water speed and blurred oil droplets, followed for a short period.

3.2 Standing tank

Design

Grammeltvedt (2013) unveiled a need to investigate the development of a droplet distribution based on rising speed alone. To investigate this a standing tank was built. The tank had dimensions as seen in figure 3.5 A pump was connected to a loop of hoses in order to circulate water and inject oil into the tank. The current of the pump could be adjusted to achieve the desired water flow. A separate tank filled with coloured oil was connected to the water stream. Overpressure was applied to the oil tank by an air compressor. The amount of oil injected into the water stream could be adjusted by a valve at the inlet to the water stream. The inlet for the water was placed on the lower part of the side wall. Based on initial testing a relatively high water flow was chosen to avoid oil from rising, and thereby forming coherent droplets before entering the tank. To reduce the effect of turbulence from the flowing water on the rising oil bubbles in the

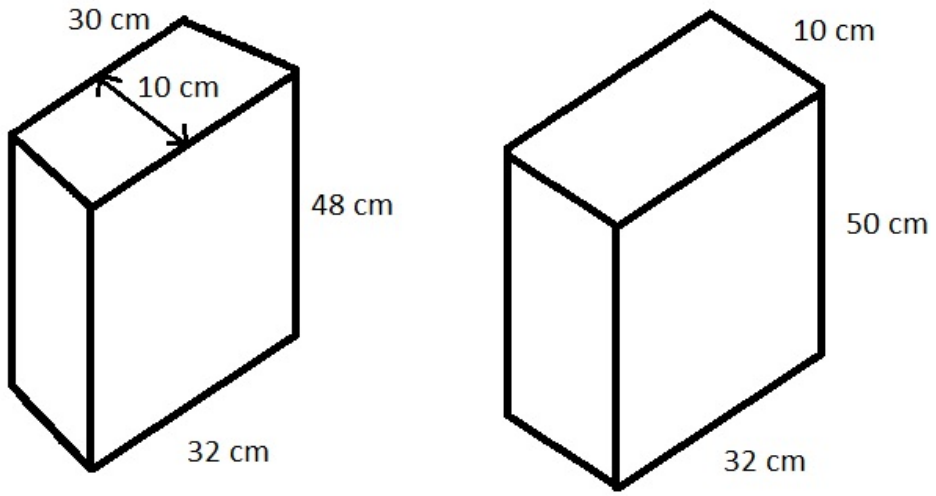

Figure 3.5: Dimensions of tank 1 (left) and tank 2 (right)

first tank, a second tank was built. The aim was to allow the water and oil to enter the tank vertically from the bottom. By doing so the author hoped to remove the effect of oil rising within the water stream before the inlet and allowing use of a reduced water flow. Schematics of the two tanks can be seen in figure 3.6. After some testing it was discovered that the valve used to disperse the oil into droplets was probably not functioning as intended. The valve used was a "globe valve" which can be seen in figure 3.7. Rather than injecting dispersed oil into the flowing water stream the oil most likely was dampened when spraying upwards inside the valve and the observed oil dispersion was an effect of the water turbulence as the oil slowly flowed into the water stream. Therefore a nozzle was manufactured to inject oil with a direct jet stream. The nozzle was designed to fit inside the tube from the oil tank. The opening in the nozzle was based on some back of the envelope calculations using Bernoulli's equation.

$$\Delta p = \frac{1}{2}\rho v^2 \tag{3.1}$$

Based on a expected injection rate of one litre/hour this gave a desired diameter of 0.2 mm. However the smallest drill bit at hand was 0.4 so this was the value which we settled for. The

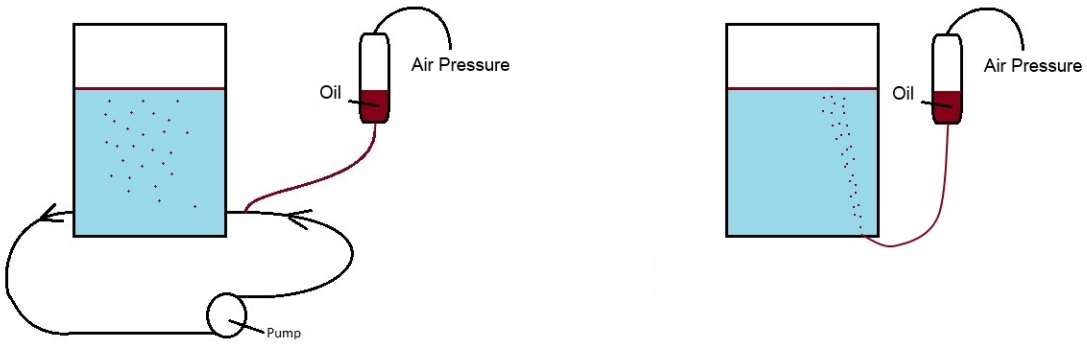

Figure 3.6: Schematic for the two tanks. Tank 1 on the left with inlet and outlet placed at opposite sides. Tank 2 to the right with inlet at the bottom

nozzle was designed as a hollow plastic cylinder with a small hole at the injecting end. At first attempts were made to inject from this nozzle into the water stream. However oil would not flow through the nozzle. After cleaning out any particles blocking the nozzle it was tested freely under water. The spreading of oil was deemed so successfully that further testing was conducted with oil being injected into the tank directly through the nozzle, thereby avoiding water circulation completely. Picture 3.8 show the oil flowing through the nozzle into the tank.

Experiment description using valve

The first tests were conducted in tank number 1. This thank had a horizontal inlet and a relative high pump voltage was used achieve a high water speed in order to reduce entry time for the oil into the tank. This was done to reduce the time for the oil could rise before reaching the inlet. Some inlet effects had to be expected as the pipe narrowed at the connection to the tank. The speed of the flowing water carried some of the oil inside the water stream all the way across the tank to the outlet for the water stream. The largest oil bubbles started rising at about the middle of tank when the oil droplets rose out of the high current water stream. A somewhat even distribution could be observed all the way to the end wall at the outlet. Tests was conducted at two different oil pressures 0,5 bar and 1,0 bar. Attempts were made to keep water level constant at 35 cm above bottom, equivalent to 30 cm above the inlet. Tests were conducted at flowing conditions by taking several images from a fixed location. The images were then analysed to account for uncertainties in the spreading of the oil droplets and fluctuations in the water stream.

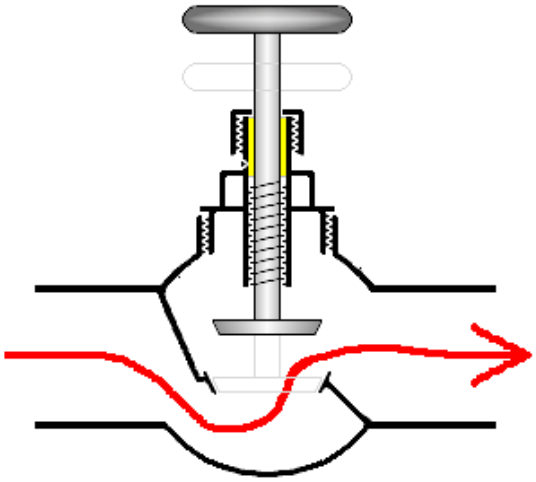

Figure 3.7: Schematic of a globe valve. (Adapted from Padleckas (2006))

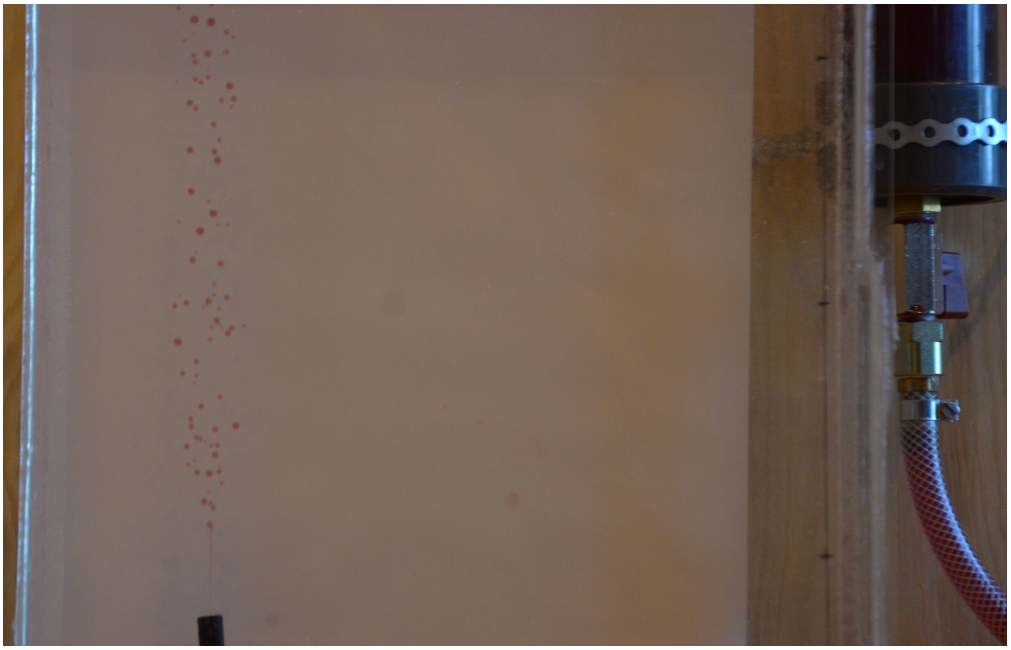

Figure 3.8: Image from testing in tank 2. Oil is injected with a pressure drop of 0.8 bar through the nozzle at the bottom. Air pressure is applied to separate container on the right,

A second set of test were conducted by shutting in the flowing oil and taking continues images at 3 frames per second to study the development of the droplet distribution as the oil rose. After building a new tank a similar set of experiments was conducted in the second tank. At first the oil was introduced into the tank without flowing water to see if a droplet distribution could be achieved directly from pressure difference across the valve. Unfortunately the oil and water properties along with the inlet distance form the valve to the tank allowed the oil to form into one single stream and probably breaking up only based on stability criteria consideration. Another set of of experiments was therefore conducted with water leading the oil vertically into the tank. The experiments were conducted with varying pump voltages to determine the required rate of water to carry the oil into the tank in the same droplets as the valve induced.

Experiment description using nozzle

After observing that oil droplets was increasing in size with increasing pressure. It was deemed that the valve was not working as intended. A nozzle was therefore manufactured. During initial testing some problems regarding particles blocking the opening was encountered. When these were fixes experiments wre conducted by injecting oil through the nozzle, only driven by air pressure applied to the oil inside the cylinder tank. The experiments were varied by altering the air pressure exerted onto the oil and by injecting both horizontally trough the side wall and vertically from the bottom. Two types of tests were run as for the valve. The first test was taking images of the droplets at flowing conditions. This was done to compare the droplet distribution resulting from the pressure loss across the nozzle. The injected oil could first be observed as thin single stream flowing into the tank. As the oil was slowed by the water in the tank the stream split into droplets. An example of the resulting stream and droplets for injecting horizontally with a pressure drop of 0.8 bar can be seen in figure 3.9. The second test was conducted by taking continuous images at three frames per second to study the rising speed of selected droplets and the development of the distribution with time. The flow was stopped by quickly shutting a ball valve on the tube connecting the oil tank to the nozzle in the water tank. For these experiments two different oils were used. One vegetable oil consisting of a mix of soy and olive oil, the same kind used for cooking, and one paraffin, Exxol D60. The measured oil properties can be seen in table 3.4.

Figure 3.9: Image of oil injected horizontally trough a nozzle with a pressure drop of 0.8 bar

	Density	Viscosity	Interfacial tension with tap water
Vegetable oil	913.4 kg/m^3	52.1 cP	21.5 mN/m
Paraffin	791.1 kg/m^3	0.80* cP	15.15 mN/m

Table 3.4: Oil parameters, measured at 22.5 °C

3.3 Images

Photography and camera settings

An important part of the experiment was to take pictures for image analysis. For details on photography regarding test conditions one to six in the wave flume see Grammeltvedt (2013). For the standing tank and adapted wave flume experiments Nikon D7000 camera was used. The camera was placed on a rack as far away from the subject as possible and zoomed in optically using a telephoto lens (105mm f/5.6). For the standing tank, a 500 watts lamp was used to balance the natural light from the windows in the test hall, but no direct light was used. For the wave flume experiments Two 500 watts lamps placed at a 90° angle, shone through a thin sheet of matt paper at the back wall. Each lamp was placed in a box coated internally with matt black paint to reduce the amount of reflection and to get parallel light waves in the pictures. A schematic of the flume and photography set up can be seen in figure 3.10. The camera was focused in the middle of the flume. To get sharp images short shutter time was prioritized with a fixed value of 1/125 second. Because of the relative short width of both the flume and tank the largest available aperture was chosen to give maximum light for the images. Finally to ensure stable conditions for each test the ISO value was set to a fixed value, which gave a satisfactory saturation. For shut in experiments and the runs in the wave flume image series were taken with a frame rate of three images per second.

Image analysis

Before the image analysis could start lopsided pictures were rotated using the program ImBatch. Then all the pictures for a given experiment were cropped simultaneously using Microsoft Office Picture Manager to get the same excerpt. Usually areas with even colour in the background and even saturation were chosen to enhance repeatability. After cropping the images were processed in ImageJ. Here the contrast was enhanced using the function "subtract background". Different values for "rolling ball radius" in this function could be applied based on how sharp the images were and how small droplets we wanted to identify. When the background was subtracted the pictures were binarized using the automated function "make binary". This function chose an

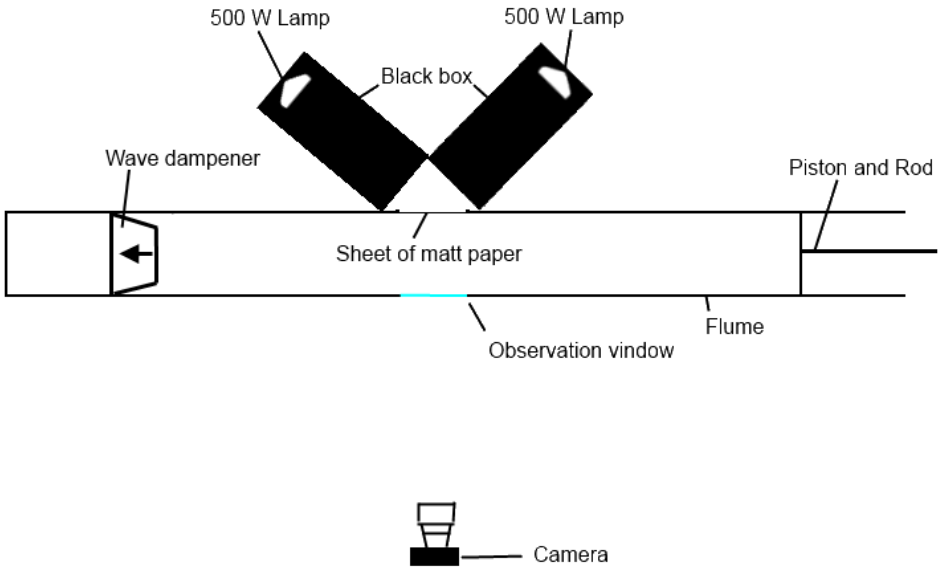

Figure 3.10: Schematic of the set up for taking pictures

automatic threshold value and removed all parts of the images which was lighter than this value. Finally an algorithm for splitting partially overlapping droplets called "watershed" was applied. Example of the steps in ImageJ can be seen in figure 3.11. All of these functions was applied by an automated script before the images were ready for analysis of the droplets. For the final droplet analysis a function called "Analyse Particles" was run. The function identified all droplets larger than a chosen value 0.5 mm^2. Area and maximum and minimum feret diameter was recorded for each droplet. The results were then saved in in excel file.

Script

Each of the result files was run in a matlab script that estimated the volume of each droplet based on the geometry described in chapter 2.2. The script then sorted the droplets based on rising size. The measured droplet distribution is defined as the sum of droplets up to volume V_d divided by the total droplet volume V_{tot}. Mathematically expressed as:

$$F_m(V_d) = \frac{1}{V_{tot}} \sum_{i=0}^{i=d} V_i \tag{3.2}$$

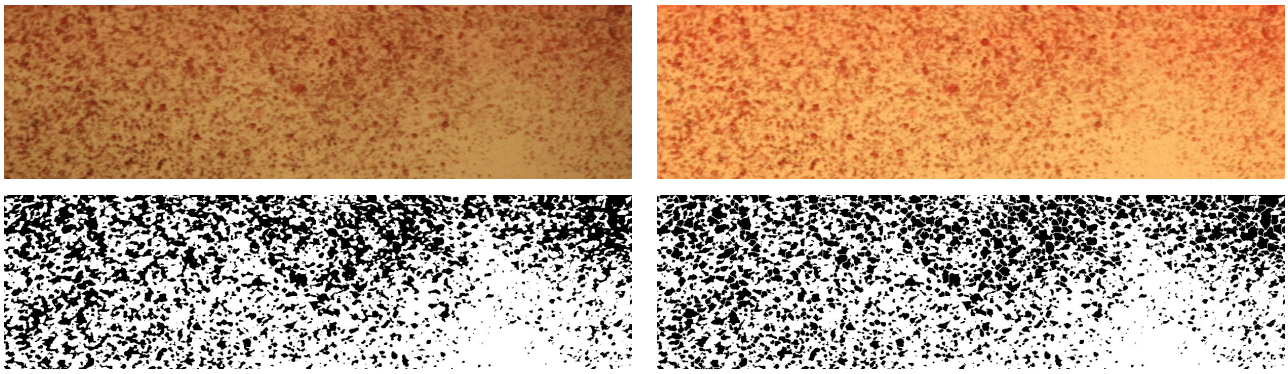

Figure 3.11: Steps in the image processing. Top left: Original cropped picture. Top right: Background subtracted. Bottom left: Made binary. Bottom right: After "Watershed", the picture is ready for droplet analysis

This gives a cumulative distribution. Asheim and Zsolt (2012) used a log-normal distribution to mathematically describe the droplets. The distribution is relatively simple and defined by only two parameters. The density function of the distribution in equation 3.2 is given by the derivative:

$$f_v = \frac{dF_v}{dV} \tag{3.3}$$

For the wave flume experiments values some key statistical values from the measured data was stored. Amongst these were:

- Number of droplets
- total droplet volume
- median
- standard deviation
- Scale and location parameter for the Log-Normal distribution

For the standing tank tests we were also interested in the actual size of droplets. In addition to saving the values for the log-Normal distribution, values for the largest and the smallest droplets were stored. These values were estimated by discarding the five largest values to account for any overlapping droplets, and then averaging the next ten values to indicate the average volume of

the largest droplets present. To account for noise generated by shadows in the background a similar approach was used when studying the smallest droplets. Discarding the five smallest ones and using the average values for the next ten as an indication for the smallest droplets.

Chapter 4

Results

4.1 Standing Tank 1

Valve, Horizontal inlet

The initial testing of the standing tank experiments were conducted with a horizontal inlet. Oil were injected into the water stream through a vale. Two different oil pressures of 0.5 and 1.0 bar was applied. The valve was opened about a quarter turn and kept in the same position for both pressures. Water was circulated with a steady pump voltage of 13.0 V. For a pressure drop of 0.5 bar, the average droplet volume varied from approximately 23 mm^3 down to 10 mm^3 with a decreasing trend. The decrease with time was expected due to smaller droplets rising slower than large ones. For 1.0 bar the average droplet volume was somewhat higher varying from about 27 mm^3 to 10 mm^3. Other values can be seen in table 4.1. Avg. $V_{d,min}$ and Avg. $V_{d,max}$ was found by ignoring the five smallest and largest droplets in each image, to remove effects from noise and coherent droplets. Then averaging the volume of the next ten smallest and largest droplets in each image. The observed increase in droplet size with pressure is opposite from what was expected from the theory. We suspected that this was a result of inlet effects and therefore proceeded to build a second tank with a vertical inlet.

Pressure bar	No. Images	Avg. No. droplets	Avg. V_d mm^3	Avg. $V_{d,min}$ mm^3	Avg. $V_{d,max}$ mm^3
0.5	11	51	16.0	1.6	31.8
1.0	12	66	16.6	1.3	37.3

Table 4.1: Results from testing in tank nr 1 using the valve and flowing water

Pump Voltage V	Pressure bar	No. Images	Avg. No. droplets	Avg. V_d mm^3	Avg. $V_{d,min}$ mm^3	Avg. $V_{d,max}$ mm^3
10.5	0.5	20	43	16.2	2.8	27.2
10.5	1.0	20	65	22.0	2.6	47.2
11.5	0.5	24	56	15.4	1.7	32.2
11.5	1.0	25	78	19.6	1.6	44.5

Table 4.2: Results from testing in tank nr 2, using the valve and flowing water

4.2 Standing Tank 2

Valve, Vertical inlet

After building the second tank with a vertical inlet we attempted to run the oil through the valve without flowing water. What we discovered was that the oil formed in a single stream which eventually broke up into droplets clearly shaped like ellipsoids. An example image from this can bee seen in figure A.3 in appendix A Further testing was therefore done with flowing water. Again the pressure was varied from 0.5 to 1.0 bar, but this time different pump voltages was also tested. As seen in table 4.2 we once again observed an increase in droplet size with increasing pressure drop across the valve. It was therefore assumed that the valve was not functioning as intended. The differences in observed values for each pump voltage strengthened the theory that the dispersion was an effect of water turbulence rather than pressure drop across the valve.

Nozzle, Horizontal inlet

The nozzle had a measured diameter of 0.4 mm. For these experiments vegetable oil with properties as given in 3.4 was used. The water level was static at 40 cm, neglecting the influence of the oil layer forming on top of the water. Estimating dimensionless length and with of the jet stream proved difficult. Varying V_d in equation 2.3 from 25 to 470 based on the length measured

Pressure bar	No. Images	Avg. No. droplets	Avg. V_d mm^3	Avg. $V_{d,min}$ mm^3	Avg. $V_{d,max}$ mm^3
0.6	9	91	8.6	1.4	17.5
0.8	7	167	11.5	1.8	27.5
1.0	8	66	6.3	0.6	24.5

Table 4.3: Results from testing in tank nr 2, injecting oil horizontally through the nozzle

from the images, this should give oil droplets with a diameter in the range of 0.015 to 0.05 mm for a pressure drop of 0.6 bar. For a pressure drop of 1.0 bar the expected droplet diameter is in the range of 0.013 to 0.036 mm. Results from the image analysis can be seen in table 4.3. The images for 0.8 bar were quite unfocused and therefore the the droplets appeared larger then their actual size after the image had been binarized. The purely empirical interpretation of the droplets is that their size fits well between those from 0.6 and 1.0 bar. Example images can be seen in appendix A. Apart from errors for 0.8 bar pressure drop, the average droplet volume show a clearly decreasing trend with increased pressure. Regarding the distribution of droplets the, log-normal distribution suggested by Asheim and Zsolt (2012) could also be applied to describe the distribution resulting from injection through a nozzle using only two parameters. Some deviations were observed, especially for the largest values, but all in all the fit was not too bad. An example of the distribution compared to the log-normal distribution can be seen in figure 4.1. This is a plot generated by matlab, using the results from one image taken at a pressure drop of 1.0 bar.

Nozzle, Vertical inlet

With the nozzle pointing upwards the droplets spread less throughout the width of the tank. For the horizontal inlet the droplets spread over a width of approximately 75 mm at a pressure drop of 0.8 bar. For the vertical inlet the spread was only about 35 mm. One way to interpret this is that for the horizontal inlet the droplets spread throughout the width of the channel and hardly anything perpendicular to the injection stream. For the vertical inlet the oil probably spreads like a cone or throughout a cylindrical volume. This could mean that the rising speed of the droplets is more likely to have a plume effect, dragging the surrounding water upwards. Average values for for testing with a vertical inlet is presented in table 4.2. The slightly higher

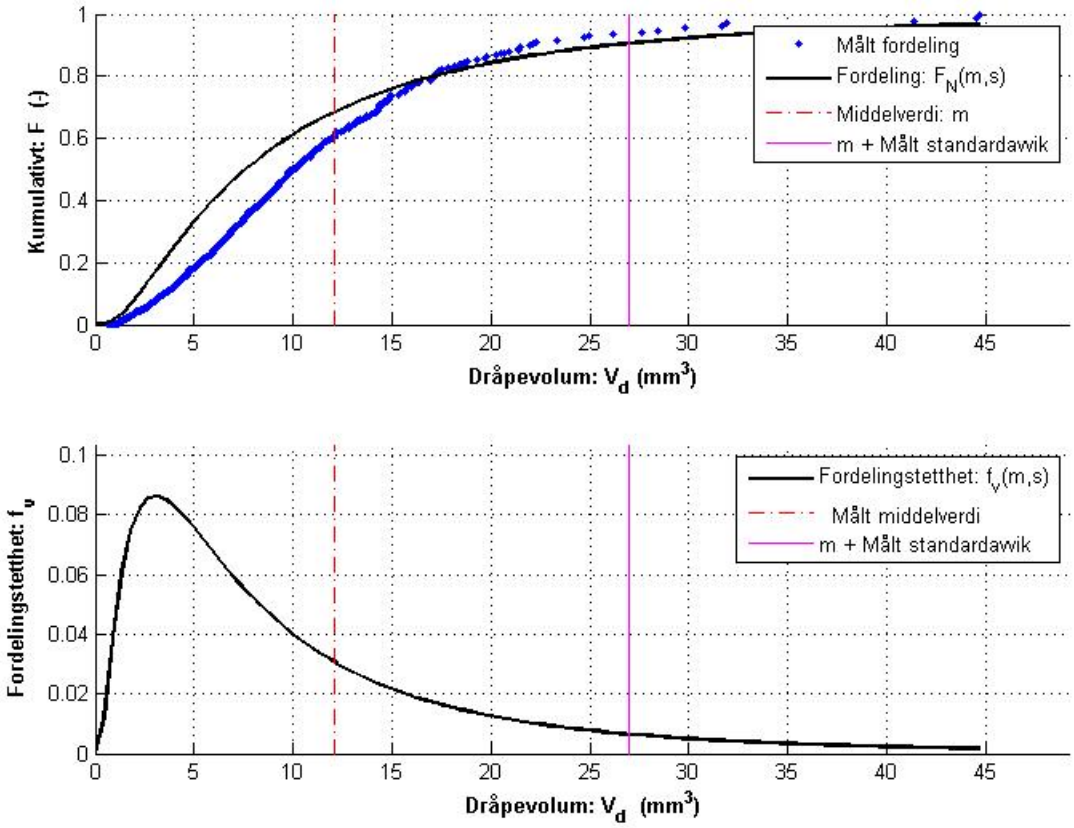

Figure 4.1: Horizontal injection, with a pressure drop of 1.0 bar. Top: plot generated from matlab of measured distribution compared to the adapted distribution using log-normal approximation. Bottom: Density distribution for log-normal approximation

Pressure bar	No. Images	Avg. No. droplets	Avg. V_d mm^3	Avg. $V_{d,min}$ mm^3	Avg. $V_{d,max}$ mm^3
0.6	9	32	9.2	4.0	11.9
0.8	10	53	7.8	1.9	13.4
1.0	7	90	6.6	1.4	13.3

Table 4.4: Results from testing in tank nr 2 injected vertically through the nozzle

values for average volume using a vertical inlet could imply that some viscosity effect is present when forming droplets in the water. The average number of droplets in each image represents the size of the excerpt used for image analysis. As the lighting was slightly different for each image the size of the excerpt varied to some extent between the different image series, to get the least amount of disturbance in each picture. This number should therefore not be used as to quantitatively describe the amount of oil flowing, but rather indicates the basis for the data. One could also discuss that the basis for describing the largest and smallest droplet volume is to small using the previous described method when the sample data for 0.6 bar only contains 32 droplets in each image on average.

Paraffin, Exxol D60

To investigate effects of density and viscosity the injection tests were repeated with other substances. Another oil, Exxol D60 paraffin with properties shown in table 3.4 was tested. At first pressures between 0.5 and 1.0 bar was applied, but to be able identify single droplets in the images pressures had to be reduced to 0.1 to 0.3 bar. For these given pressures and the same range for V_d as used for vegetable oil, the expected droplet diameters ranged from 0.015 mm to 0.25 mm. Determining the size of single droplets was difficult due the amount of droplets and the distances between them. This combined with the lack of contrast and blurry images caused the automated image handling to fail in identifying single droplets. Based on perceived size of selected droplets, the diameter were varying between 0.8 and 1.0 mm for droplets generated by a pressure drop of 0.1 bar. At a pressure drop of 0.2 bar identifying single droplets became more difficult, whilst still possible. Selected droplets were measured at diameters varying in the range of 0.7 to 0.9 mm. See example image in figure 4.2. For pressure drops of 0.3 bar and higher the oil came out in a cloud and identifying single droplets was next to impossible.

Figure 4.2: Example image from injecting paraffin with a 0.2 bar pressure drop, shortly after opening the oil flow. Single droplets can be identified, but due to the relatively dense distribution the automated image analysis failed

Air

Attempts were made to measure bubble distribution for air bubbles as well, injecting directly from the compressor. The air flow proved to be too big for nearly all pressures, creating a diverse droplet distribution with a lot of elongated bubbles. At low pressures compressor could not deliver a steady stream of air and the flow was fluctuating. Lighting was a big issue in these images as the air, unlike the oil, could not be coloured for contrast. The best images was achieved with lighting from the top, see figure 4.3. This created bubbles lighter than the background. For a pressure drop of less 0.1 bar the air flow gave a narrow column where the diameter of spherical bubbles were ranging from 1.0 to 4.5 mm. Some elongated bubbles could still be observed. Further measurements with air was not emphasized.

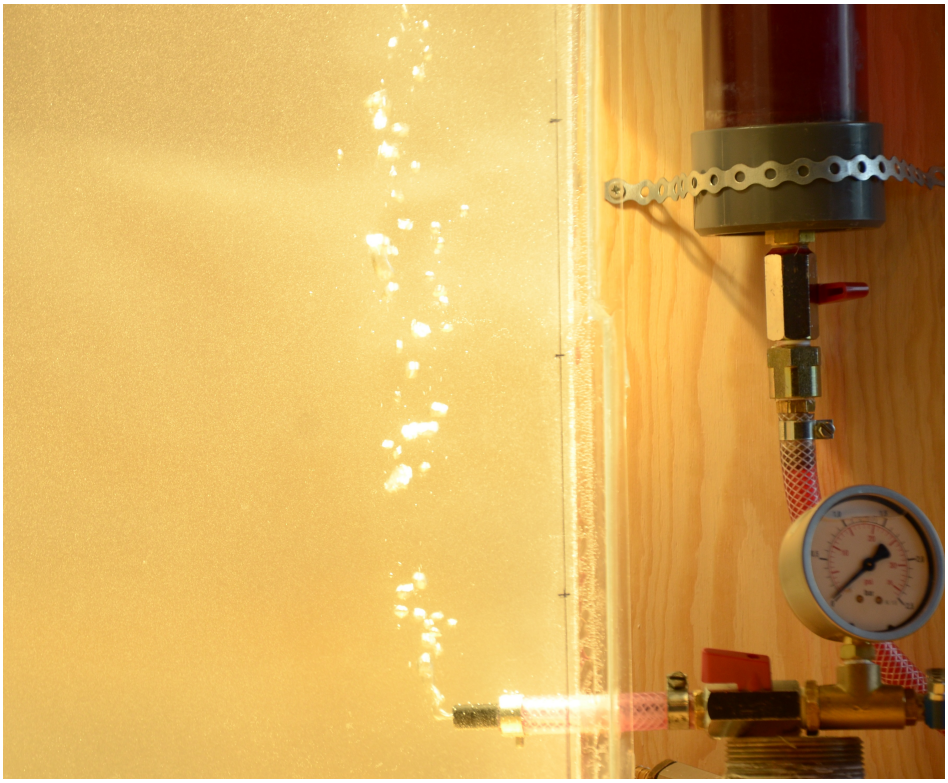

Figure 4.3: Example image from tests with air injection

4.3 Shut in tests

Shut in test was carried out to study the rising speed of single droplets and development of the droplet distribution. The rising speed experiments can be compared with linear theory for a droplet rising alone to determine any plume effects. Another way of looking at plume effects was studying average density inside and outside the plume. The method for analysing droplet distribution was choosing a small horizontal test section for each image. With a vertical spread of 5.0 mm no sorting effect for the droplets across this area was assumed. For the lowest pressure drop of 0.6 bar the sample size regarding number of droplets was a bit low for conducting droplet distribution analysis. The development of the average volume after shut at injection of 1.0 bar can be seen in figure 4.4. When estimating rising speed of selected droplets, three consecutive images were studied. Droplets which were easy to identify based on size, colouring or position were chosen and their height, relative to a fixed position was measured. Based on a frame rate of 3 fps. The velocity could be approximated. Diameter for the droplet was then measured and theoretical rising speed based on Stokes law calculated accordingly. The resulting data, presented in table 4.5 was quite surprising. Significant plume effects was not expected as the average density of all the fluid inside section with rising oil was found to be less then 1 % different from the water density. However it was not expected that the observed rising speeds would be so much lower compared to the theoretical ones. The measured droplets were endeavoured to be representative for the rest of the droplets, whilst still standing out enough to be identified in three consecutive images. When measuring the diameters it was found that the droplets had a tendency to be somewhat flatten with an elliptical shape. This together with inter facial tension effects from the surrounding water could explain some of the results. Further it should be noticed that the difference from the expected speed was increasing with increasing size. Whilst there was a visible difference in the rising speed for small compared to large droplets, the difference was perhaps less then expected. It could be that the wake from larger droplets increases the speed of small droplets rising underneath it thereby inducing a plume effect. It could also be that larger droplets have trouble overtaking small ones because of the movement in the water. With Reynolds number ranging from 90 to 300 for the selected droplets, laminar flow regime is dominant. The data from testing with the valve was not emphasized.

Horizontal inlet				
Pressure bar	Diameter mm	Velocity measured m/s	Expected Velocity m/s	$V_{measured}/V_{expected}$
0,6	3,4	0,093	0,546	0,17
0,6	1,5	0,053	0,106	0,49
0,8	2,5	0,090	0,295	0,31
0,8	2,1	0,066	0,208	0,32
1,0	2,0	0,066	0,189	0,35
1,0	2,0	0,071	0,189	0,37
Vertical inlet				
0,6	3,5	0,100	0,578	0,17
0,6	1,9	0,046	0,170	0,27
0,8	2,0	0,050	0,189	0,26
0,8	2,6	0,078	0,319	0,24
1,0	1,5	0,054	0,106	0,51
1,0	1,8	0,066	0,153	0,43

Table 4.5: Results from rising speed measurements

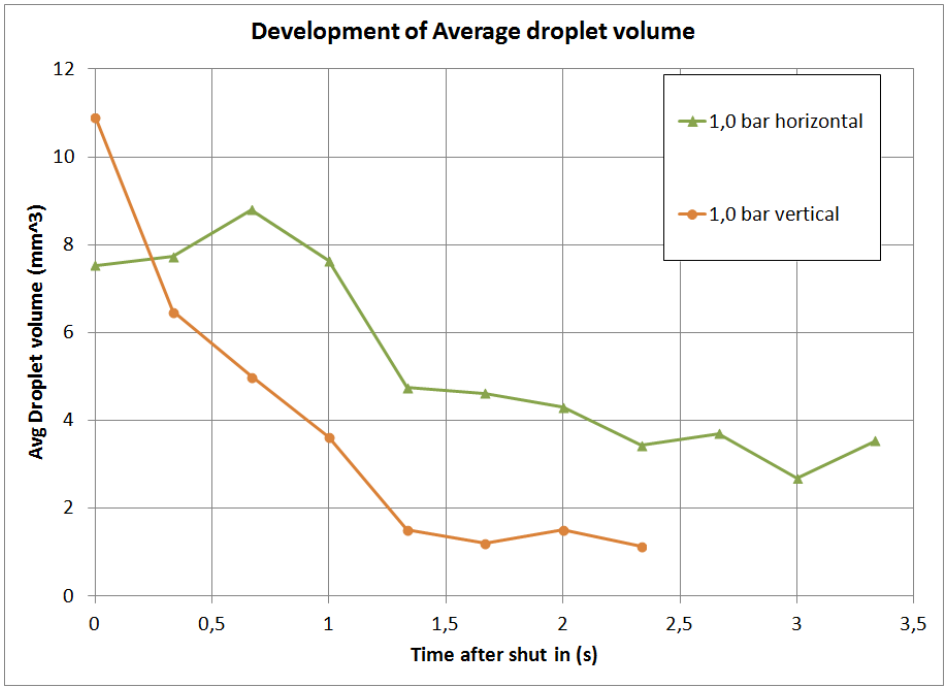

Figure 4.4: Average volume of droplets vs time after shut in for injection at 1.0 bar

4.4 Wave flume

All the experiments in the wave flume were conducted with coloured vegetable oil. The oil had a measured density of 913.4 kg/m^3 and other parameters shown in table 3.4. The observation window used was located 4 m from the piston. Oil was poured onto the water surface between the piston and observation window. The test conditions are the same as described in table3.3. Blurry images was excluded from the results because any measurements there obviously were distorted.

Test condition seven

This was the first of the test runs and the oil had not yet been properly distributed throughout the flume. Therefore the wave carried the oil past the observation window and dispersed oil droplets was first visible after the return wave had passed at about 9 seconds. There was still some motion in the water from waves passing back and fourth in the flume between 9 and 12 seconds. The droplet distribution seems to reach a quite uniform distribution after 12 seconds. From about 17 seconds a stable average volume at a value of 0.75 mm^3. This gives a diameter of 0.5 to 0.6 mm and correlates well with what could be measured in the images. Equation **??** gives a rising speed of 14.8 mm/s. With a water level of 15 cm the time for droplets to rise all the way to the surface would be in the range of 100 seconds. Considering turbulence in the water and reflected waves present in the flume this could explain that these droplets stays dispersed throughout the duration of our experiment. The development of a constant average droplet volume could also represent the sensitivity of the image analysis. Droplets smaller then 0.5 mm^2 was ignored to reduce the influence of noise due to lighting and saturation. Plots of the development of average droplet volume and scale parameter of the log-normal distribution can be seen in figure 4.5 and 4.6. The average droplet volume represents the actual size of the observed droplets while the scale parameter indicates the deviation in the measurements.

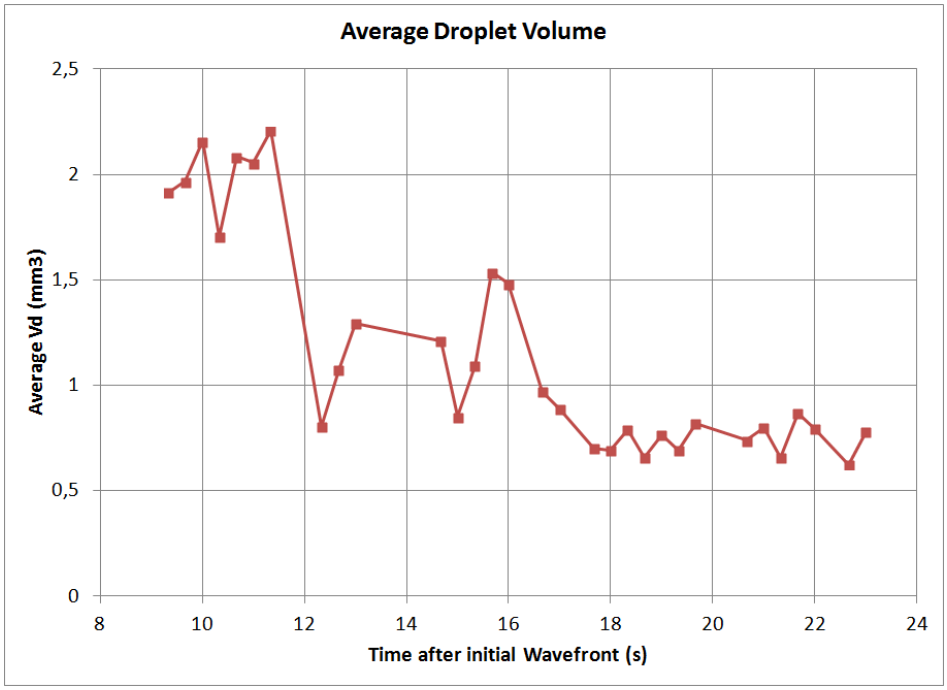

Figure 4.5: Average volume of droplets vs time after wave front for test condition seven

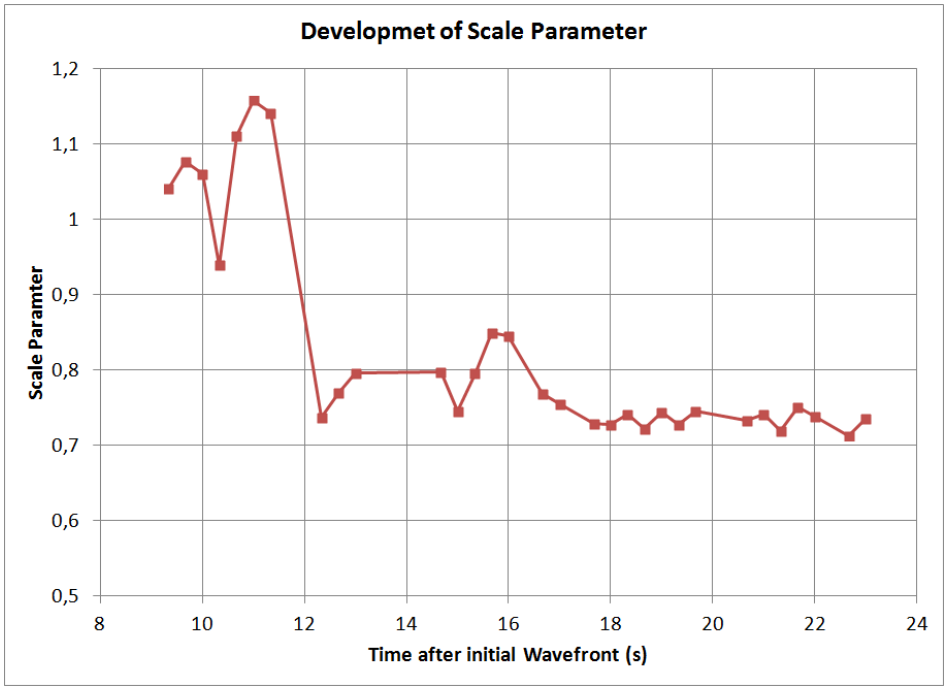

Figure 4.6: Log-normal scale parameter for droplets vs time after wave front for test condition seven

Test condition eight

This test condition is the same as Asheim and Zsolt (2012) condition number six. Similar problems to test condition seven was experienced, namely that only parts of the observation window had dispersed droplets after the initial wave had passed. The average volume shows a decreasing trend as the larger droplets rises to the surface during the period in between the initial wave and the return wave. The increase in average droplet size between four and six seconds could be because of more droplets flowing into the area of the observation window. After the return wave passes at seven seconds, more fluctuating data are observed. From the images several patches with higher droplet density passes by the observation window. This together with effects from blurred images can explain some of the inconsistency in these results. Average droplet volume at the termination of the experiment is close to that for test condition seven.

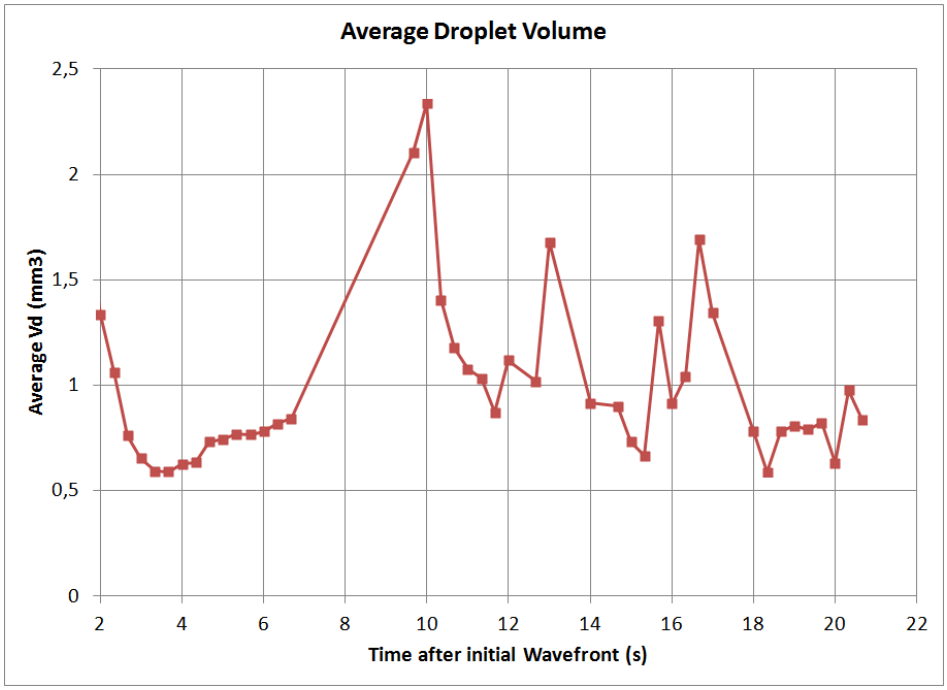

Figure 4.7: Average volume of droplets vs time after wave front for test condition eight

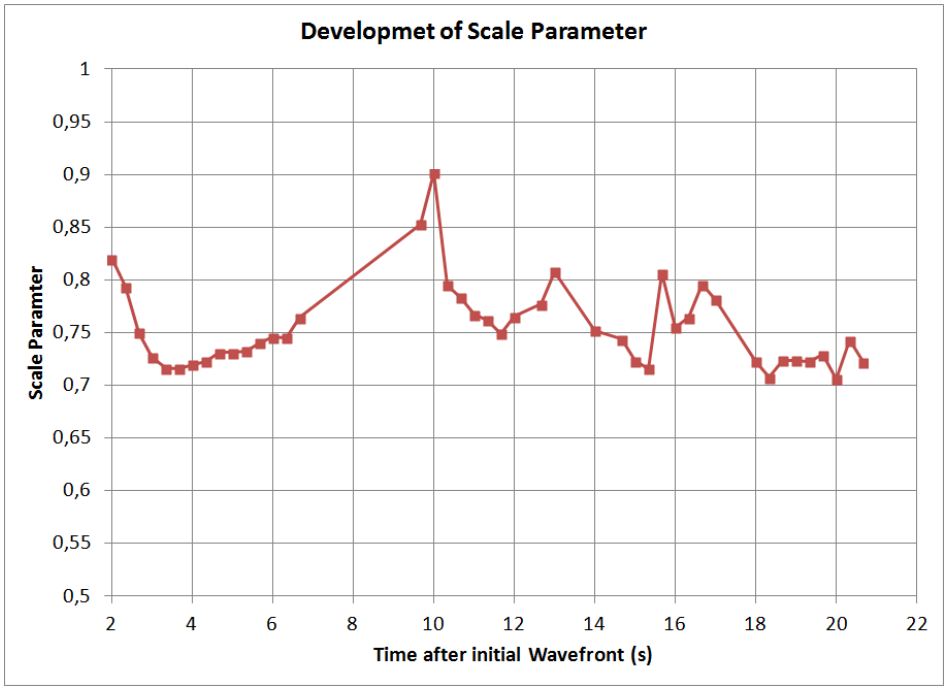

Figure 4.8: Log-normal scale parameter for droplets vs time after wave front for test condition eight

Test condition nine

This test condition is similar to to test condition one from Asheim and Zsolt (2012) analysed by Grammeltvedt (2013) but with lower piston speed. Reduced piston speed was chosen to reduce the amount of overlapping droplets and to be able to compare this experiment with condition seven and eight based on static water level alone. Three runs were made to give a better foundation for the data. Some additional oil was added to the section between the piston and observation window after each run, to account for oil been trapped behind the wave dampener. The droplet density in this experiment was still somewhat patchy with the largest droplets grouped in clusters, but smaller droplets were distributed fairly even across the width of the observation window. With the exception of some return waves passing between 4 and 6 seconds and again from the piston side between 10 and 14 seconds the data seems quite consistent. Looking at the initial section from 2 to 6 seconds after the first wave passes and before the wave returns, a decreasing trend can be observed for all runs. The average droplet volume for these runs converges towards a average value of approx. 0.5 mm^3 equivalent to a diameter of 0.5 mm. This value corresponds to a slightly higher value than the limit set at 0.5 mm^2 or a diameter of 0.4 mm. Still the data is quite close to the sensitivity for the image analysis. As a result one could perhaps expect the average to drop further. The difference in value for converging droplet volume towards the end of the image series for the different experiment conditions, can perhaps be explained as a result of the dispersion force generated by the wave. According to (Asheim, 2011) dispersion force is increasing with increasing Froude number. The Froude number is linked to the wave hight compared to static water level. With a larger Froude number smaller droplets for test condition nine is expected compared to condition seven and eight.

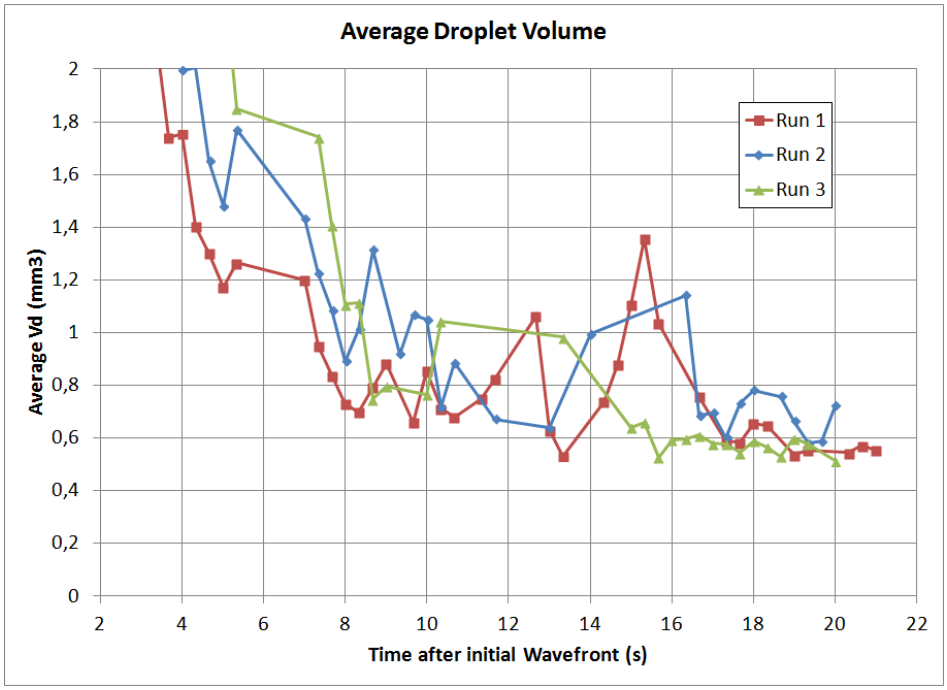

Figure 4.9: Average volume of droplets vs time after wave front for test condition nine

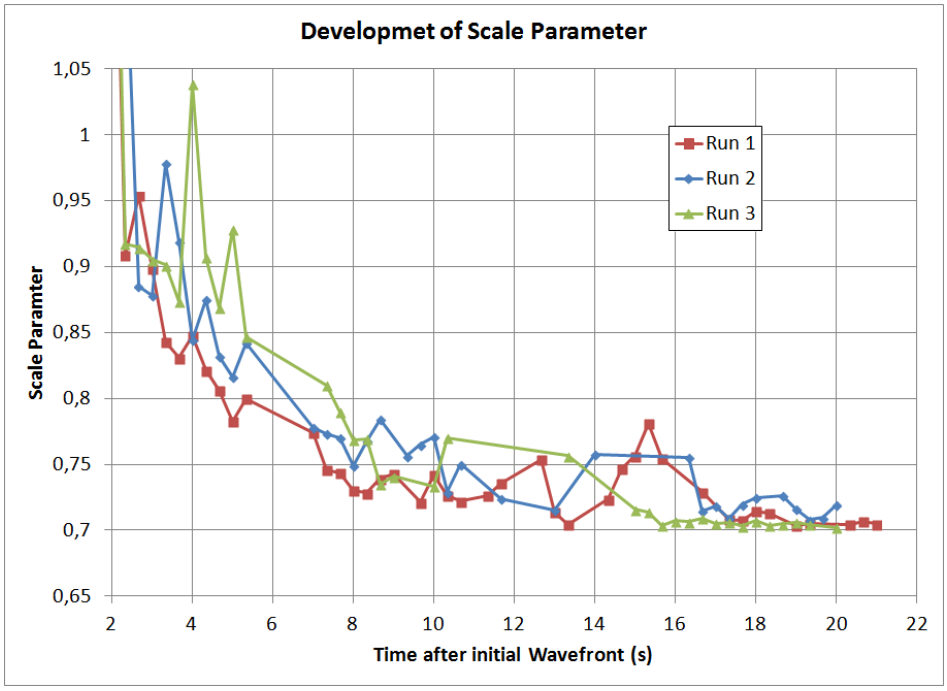

Figure 4.10: Log-normal scale parameter for droplets vs time after wave front for test condition nine

Chapter 5

Discussion

5.1 Photography

There were several issues with regards to the photography. The goal was to get clear images with as consistent conditions as possible to ensure repeatability both throughout each image series and for the different experiments.

Standing Tank

Lighting for the standing tank experiments was mostly natural. One lamp was placed opposite of the windows in the test hall to balance the light. This lamp did not shine directly onto the tank. To enhance to contrast the back of the tank had a sheet of white paper attached to it. The use of natural light resulted in parts of the images being darker due to shadows. Especially the top part underneath the surface had to be removed when analysing the images. Attempts were made to use direct light from the front of the tank, but this resulted in shadows from the droplets and had to be abandoned. Use of back light similar to what used for the flume could have given better images, but this was not tested.

Wave flume

As emphasized by Grammeltvedt (2013) lighting seems to be a particular issue. Compared to the images taken by Asheim and Zsolt (2012) much larger sections of the images taken for this

report could be used. Asheim and Zsolt (2012) used only one lamp shining directly at the back wall, which gave a brighter section in the center and darker sections towards the edges. This made using the whole image impossible as the threshold values in ImageJ will perceive the entire outer parts of the picture as oil droplets. Using a this set-up with two lamps at an angle seemed to take care of this problem, and little noise was observed in the images. The most disturbances in the images was experienced at low droplet concentrations of small droplets, and as a result the data taken at the end of each image series could be somewhat distorted by noise. In this experiment sharp contrast between the oil droplets and the water is preferable. To achieve this oil was coloured with sudan red. Naturally coloured oil could be used to achieve this effect. Reed et al. (2009) used a white screen inside the flume to enhance the contrast in their experiments, but as a result they had to position the lighting on same side as the camera. This could result in reflections from the glass affecting the images.

Camera settings

Camera settings was kept constant throughout the experiments only varying the ISO value to account for the amount of light i the images. Using fixed settings was important in order to get usable and consistent images. For these experiments the camera was set to prioritize shutter speed in order to avoid blurry images. Asheim and Zsolt (2012) used a fixed value of 1/250 s while we used 1/125 s. Since some blurry images was experienced shorter shutter speed could have been tested. When scrolling trough the image series some differences in the brightness could be observed. This is most likely due to the amount of natural light in the room in addition to the amount of dark droplets present in the images. ISO, shutter time and aperture work together in a camera to provide a correctly exposed image with regards to lighting. If the sum of these is too high the picture will be oversaturated. The camera was placed as far away from the observation window as possible. This was done to get an even focus throughout the total width of the flume, in order to avoid blurry droplets at the front or back of the image. Asheim and Zsolt (2012) used a lens with greater zoom and as a result they could stay further back from the subject. With a scale of 9.5 pixels / mm the smallest droplets was hard to measure accurately. We could have moved the camera closer to the subject or used a lens with greater zoom to increase the scale, which in turn would allow more digital zoom for each image and help improve the accuracy of

the experiments.

5.2 Image analysis

ImageJ

The major shortcomings in ImageJ was mostly related to blurry images and unevenly distributed light. Several functions were run to prepare the images for droplet analysis. The images were cropped in order to remove darker parts of the images. The function "subtract background" was applied to enhance the contrast. Using smaller values for the "rolling ball radius" in this function improved the amount of noise that was removed but it also greatly increased the time used to process each image. As a result each image series was tested to determine the effect of using a smaller value. The gain was the compared to the increase in time used to process the images. As a result smaller values was applied to image series which had the smaller droplets. Another built-in function called "enhance contrast" could have been applied, either instead or in addition to "subtract background". It was chosen to not to use this function, the reason being that it made separating droplets in darker or overlapping regions more difficult after binarization. When using the function "make binary" an automated value for the threshold was applied. This value was different for images with different light intensity. Using an automated threshold value seems like a better option than using a fixed value as it to some extent considers the overall lighting of the image. However an automated value does not take into account the shade from a droplet or effects from overlapping droplets or droplets without clearly defined edges. For our results the use of an automated value seemed to yield somewhat larger droplets then what was the reality because of the boundaries for the droplets not been clearly defined. In some cases with a high density of droplets, stand alone droplets might have been excluded because of their colour intensity with the threshold value set to auto. The final function used was the "watershed" function, used to split overlapping droplets. This algorithm also seemed to fail to some extent in dark areas or when overlapping droplets had a non-circular shape.

Matlab script

The results from different droplet analysis were run in a matlab script. The script plotted the cumulative distribution and the density function for each of the images. In addition some values were stored. Automated handling of the data allowed for more data to be processed. Making most of the image handling autonomous allows for processing of more images and thereby enables higher frame rates or longer duration for the experiments.

5.3 Standing tank

The standing tank experiments had some issues regarding the sample size for small pressure drops. With the lighting issues as discussed in the photography section and relatively low flow of oil, the variations in sample size at flowing conditions was quite large. Building a larger tank or improving the lighting could fix this. The air compressor worked fairly well, but especially at low pressures maintaining stable conditions proved difficult. We assumed that the turbulence caused by the pressure difference across the nozzle was what caused the the oil breaking into droplets and that pipe friction was assumed negligible. With results deviating quite a lot from the expected values one could in retrospect question this assumption. A quick release connection was used to connect the tube from the oil tank to the inlet. This was a spring operated locking mechanism which was opened when the tube was connected. Even though the area for oil to flow through this was greater then the area across the nozzle some of the pressure loss could have happened in this connection. Because of the low concentration of oil droplets we also assumed no plume effects for the vegetable oil. Average density inside the plume was estimated by image analysis and found to be approximately the same as for water. For the paraffin however the influence of plume effects seemed considerable based on the development of the steam as we opened the the flow. Unfortunately estimating average densities and rising speed for paraffin droplets was not possible due to their small size and dense distribution.

5.4 Wave flume

The wave flume is briefly discussed in Asheim and Sivertsen (2012). They concluded that the wave hight and speed is in accordance with existing theory and that the facility enables repeatable conditions for breaking waves. The effect of the inserted wave damper was not sufficiently satisfying with regards to reduced motion past the observation window. Other types of wave dampers was discussed but not installed due to time and space consideration during the testing. Other solutions which probably would work is to attach a wider tank at the end with a something breaking the wave towards the sides of the tank, in order to avoid the wave from returning back into the flume. Use of a deeper tank at the end could also give similar effects as the force of the wave is linked to the water depth. With regards to fluid properties coloured vegetable oil and water was used in these experiments. Other fluids will probably yield different droplet distributions. How the oil is spread across the surface of the flume also affects how evenly the oil is distributed after the wave. An even distribution is favourable to get consistent data for the development of the droplet distribution. Due to wear on the observation window we had to use a window closer to the end of the piston. This increased the time before the wave returned, but also gave quite high sideways motion just after the wave had passed. The window in itself was not ideal as some of the glass at the bottom was cowered with tape to help seal the gap between the glass and the wood. In general one would like to be able to see as much of the area underneath the water surface as possible to give a larger sample for the droplet data. The high water level from test condition seven was in this way preferable, but during testing at that water level quite a bit of the water was spilled at the wave dampener due to the force of the wave.

5.5 Data and Results

Blurry images and overlapping droplets induced errors using the automated threshold value and applying the watershed function. Based on the image analysis the smallest diameter for which single droplets were visible in the images was about 0.4 mm. Smaller droplets could be found but was not detected by the analysis. To reduce the amount of noise on the results a threshold for minimum droplet area of 0.5 mm^2 was applied. The relative error related to blurry images with droplet edges not being clearly defined was larger for small droplets. Taking images closer to

the subject or at higher resolutions could help to enhance the accuracy of the data. Because the uncertainties regarding the images are significant, qualitative values for the uncertainties are only partially included. For a droplet with perceived diameter of 2.0 mm from the images the actual value could vary as much as ± 0.5 mm based on where one would interpret the boundary. The automatic particle analysis would tend to chose the largest value. This should be considered when analysing the presented results.

Standing tank

For the standing tank images the blurry conditions are most likely an effect from the focus of the images rather then rapid movement. Use of higher shutter speeds would then not have yielded different results. The deviations from the measured results compared to the expected ones are partially discussed in the results section. For the flowing tests the resulting distribution could to some extent be described by the log-normal distribution as suggested by Asheim and Zsolt (2012) for the wave flume. Deviations from the adapted distributions were largest for the larger droplets. The resulting average values for droplet diameter were far from the expected values even with a wide range for the dimensionless diameter. It was also interesting to observe the effect of injecting horizontally and vertically. A tendency to yield larger droplets when injecting vertically indicates that how the water is slowing the stream affects the size of the droplets. For a vertical injection the stream would be slowed from above whilst more oil is being forced upwards from the bottom. This could result in larger droplets as coherent droplets merge. For the horizontal injection the droplets will start to rise some distance after the nozzle when the speed has decreased. Here flowing oil is not forced into the droplets from below. All in all this points to the inter facial tension between the oil and water having some influence to the droplet size. Looking at the droplets from injecting paraffin these were much smaller and spread more rapidly after leaving the nozzle. Even though we could not get any measurable results for these droplets it was quite clear that they were closer to the expected values.

The high deviations from expected values observed in the rising speed tests were surprising. A slightly lower then the theoretical value was expected as the droplets were somewhat elliptical. This would result in higher drag for the droplet compared to the buoyant force. To determine if

any plume effects was present, single droplet experiments could be conducted by injecting one droplet at the time from a syringe. Unfortunately there was not time to do this. The measured diameter obviously plays a major part in determining the expected value. Diameters was measured based on perceived boundaries for each droplet. Sensitivity analysis of the diameter was done for some of the droplets. Those indicated that for a droplet with a perceived diameter of 2.0 mm, a decrease in diameter by 0.5 mm or equivalent to 25 % would reduce expected rising speed with almost 45 %. This indicates that the accuracy in the measurements was not good enough for small droplets. All in all the rising speed tests indicates some effects from inter facial tension and resistance from the water is present. Unfortunately measuring the friction factor for the oil droplets in the water is difficult and was not done.

Wave flume

As expected, a decreasing trend in droplet size was observed over time for all experiments in the flume. Motion created by the return wave and the positioning of the oil on the surface before the wave passed affected with some of the images. Single occurring breaking waves is not a realistic situation for oil floating on the sea. A continuous process of mixing the oil into the water is more likely and as a result a more evenly distributed dispersion with larger droplets near the surface and decreasing size downwards should be expected. Estimating rising speed of the largest droplets proved difficult due to sideways movement and have been excluded from this report. As suggested by Reed et al. (2009) andAsheim and Zsolt (2012) log-normal distribution was chosen to describe the frequency of droplet size. An approximation in itself contains error and other distributions could have given more correct results. The log-normal distribution was chosen because of the relative straight forward mathematics and being dependent on only two parameters. It seems safe to conclude that as expected the average size of droplets decreases with time along with the total droplet volume. The converging value for droplet size in the experiment is interesting. It could represent a value for the smallest value for droplets based on the force of the wave. This could also be compared to the Weber number and expected droplet size for a given wave. However at least for test condition nine where this converging value is close to the lower limit for droplet volume in the image analysis it is more likely that this is an effect of the sensitivity of the measurements.

Chapter 6

Conclusions

The observed results and the previous discussion provides foundation for the following conclusions:

- The optic measuring system and image analysis tools functions works best for conditions with well dispersed and large oil droplets. Sharp images with clearly defined droplet edges in contrast to the water improves the validity of the results.
- To be able to use the data quantitatively a homogeneous distribution of droplets across the width of the observation window is required in the wave flume. The changes in the set-up for lighting was satisfactory, but less sideways motion is preferable
- The numerical results deviates from theoretically expected values for the standing tank. This is probably due to a combination of high viscosity for the vegetable oil, inter facial tension between the oil and water and large uncertainties regarding the actual droplet volumes compared to the measured ones

Additionally I would suggest the following for future work and improvements :

- Install an improved wave dampener as suggested, to reduce sideways motion for further experiments in the wave flume
- Repeat the tank experiments in a larger tank and with improved lighting conditions to get a larger basis for the data

- Repeat the tank experiments using other oils with parameters varying between those tested in this report
- When taking images, endeavour to take images in high resolution and close to he subject as this will allow for more digital zoom, which in turn will enhance the accuracy for small droplets

Bibliography

Asheim, H. A. (2011). Oppbryting av oljeflak i bølger. Technical report, Norwegian University of Sience and Technogy, Trondheim, Norway. Written in Norwegian.

Asheim, H. A. (2012). Notat: Dråpestørrelse etter dyse. Written in Norwegian, unpublished.

Asheim, H. A. (2013). Multiphase flow. Course notes on multiphase flow. TPG4245 - Production Wells, Norwegian University of Sience and Technogy, Trondheim, Norway, http://www.ipt.ntnu.no/~asheim/prodbr.html. Accessed: December 2013.

Asheim, H. A. and Sivertsen, A. (2012). Forsøksanlegg for brytende bølger. Technical report, Norwegian University of Sience and Technogy, Trondheim, Norway. Written in Norwegian.

Asheim, H. A. and Zsolt, V. (2012). Ny lense, rapport 2012: Dråpefordeling for olje i brytende bølger. Technical report, Norwegian University of Sience and Technogy, Trondheim, Norway. Written in Norwegian.

Delvigne, G. A. L. (1993). Natural dispersion of oil by different sources of turbulence. *International Oil Spill Conference Proceedings: March 1993, Vol. 1993, No. 1, pp. 415-419.*

Delvigne, G. A. L. and Sweeny, C. E. (1988). Natural dispersion of oil. *Oil and Chemical Pollution, 4 , 1988, 281-310.*

Dunnewind, B., Bos, M., and Koops, W. (2003). Entrainment of oil from oil spills into the water column: a new theory. *International Oil Spill Conference Proceedings: April 2003, Vol. 2003, No. 1, pp. 1059-1066.*

Grammeltvedt, E. (2013). Image analysis of dynamic size distribution of oil droplets dispersed by a breaking wave. Semester project.

Hinze, J. O. (1955). Fundamentals of the hydrodynamic mechanism of splitting in dispersion processes. *AIChE Journal Volume 1, Issue 3, pages 289–295, September 1955*.

Mercator, P. (2012). Ellipsoid tri-axial abc. http://www.en.wikipedia.org/wiki/File:Ellipsoid_tri-axial_abc.svg.

Padleckas, H. (2006). Cross-sectional diagram of an open globe valve. http://en.wikipedia.org/wiki/File:Valve_cross-section.PNG.

Reed, M., Johansen, O., Leirvik, F., and Brørs, B. (2009). Numerical algorithm to compute the effect of breaking waves on surface oil spilled at sea. Technical report, The Coastal Response Research Centre. http://rfp.crrc.unh.edu/projects/viewProject.php?PROJECT_ID=26.

Zheng, L. and Yapa, P. D. (2000). Buoyant velocity of spherical and nonspherical bubbles/droplets. *Journal of Hydraulic Engineering 126 (11), 852-854*.

Appendix A

Images from standing tank tests

Included in this appendix are several picture taken at each different test condition for the standing tank experiments.

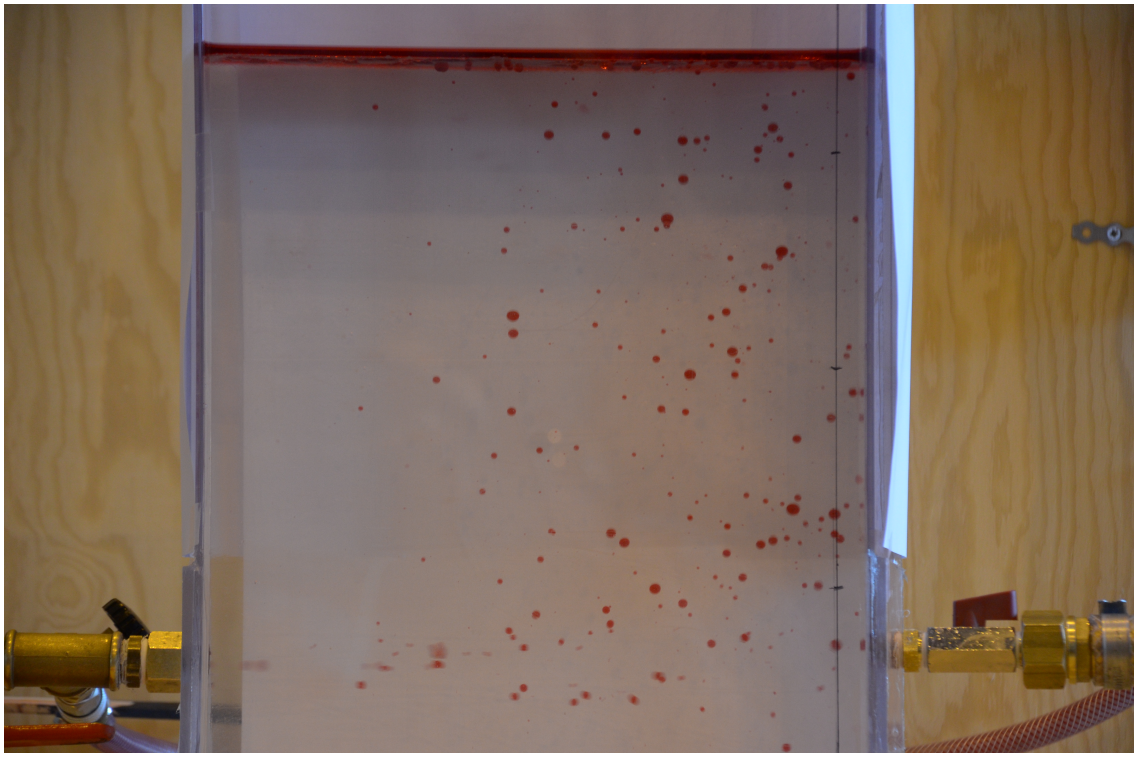

Figure A.1: Testing in tank 1 with a pressure drop of 0.5 bar across the valve and pump voltage 13.0 V

Figure A.2: Testing in tank 1 with a pressure drop of 1.0 bar across the valve and pump voltage 13.0 V

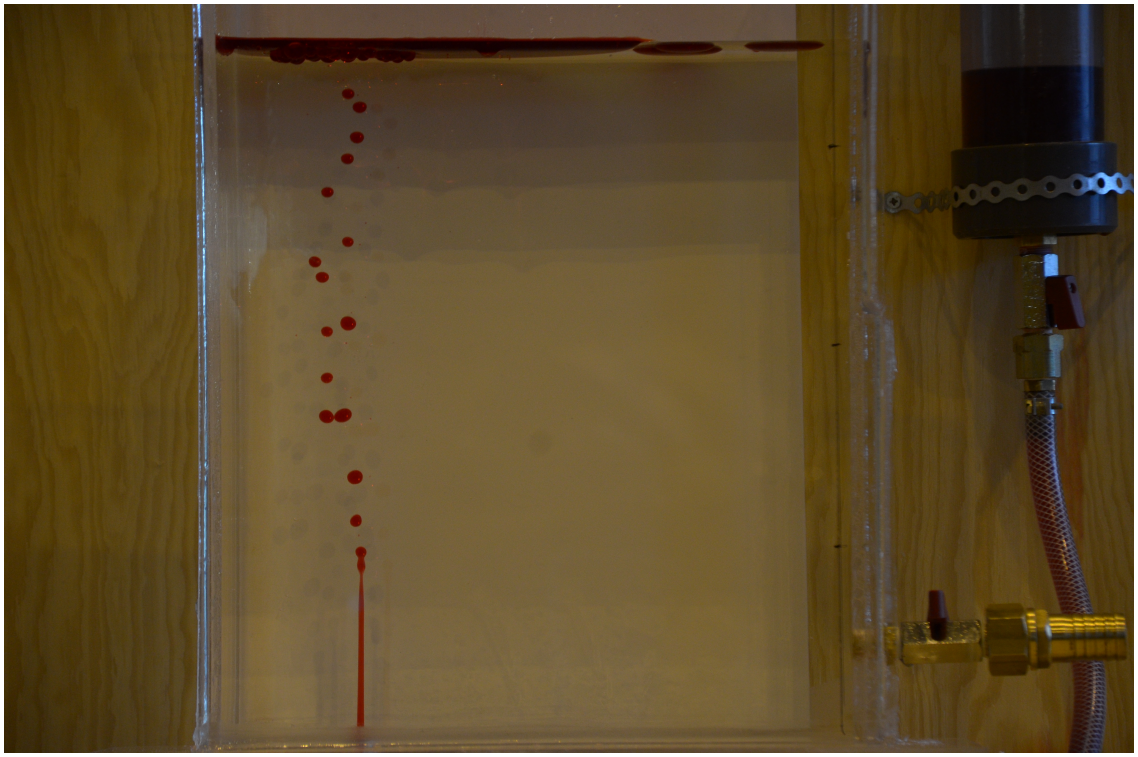

Figure A.3: Testing in tank 2 with a pressure drop of 0.5 bar across the valve and without flowing water

Figure A.4: Testing in tank 2 with a pressure drop of 1.0 bar across the valve and without flowing water

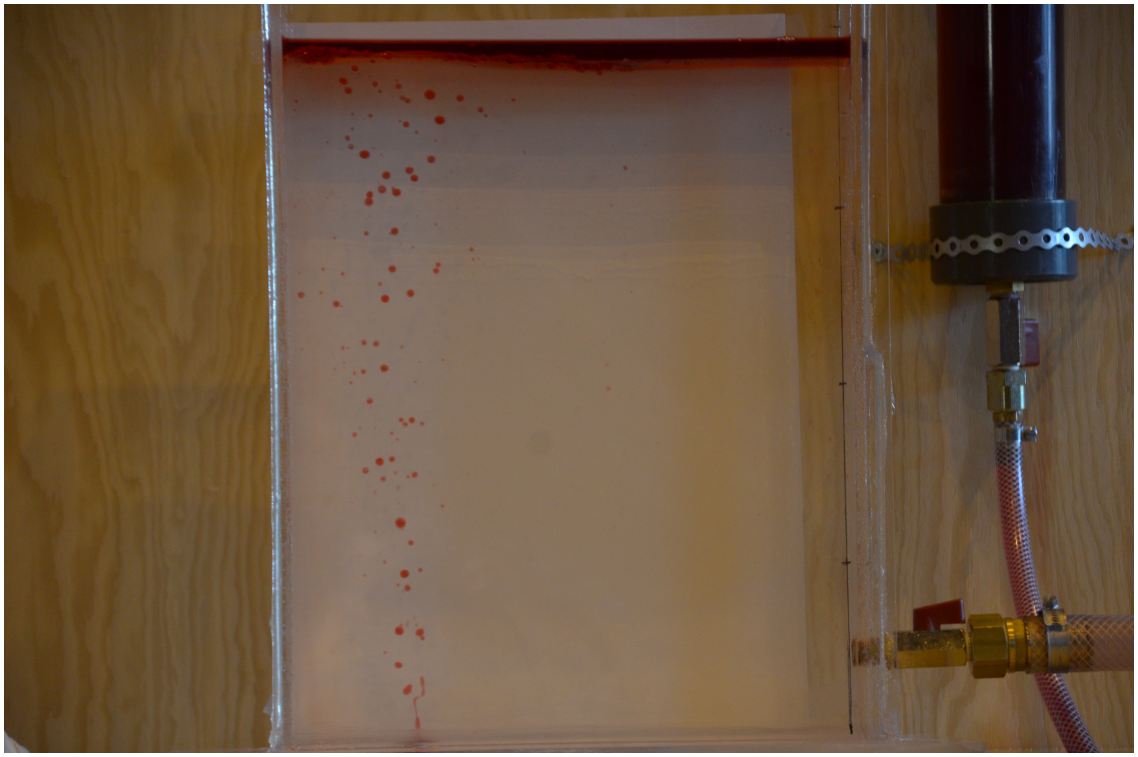

Figure A.5: Testing in tank 2 with a pressure drop of 0.5 bar across the valve and pump voltage 10.5 V

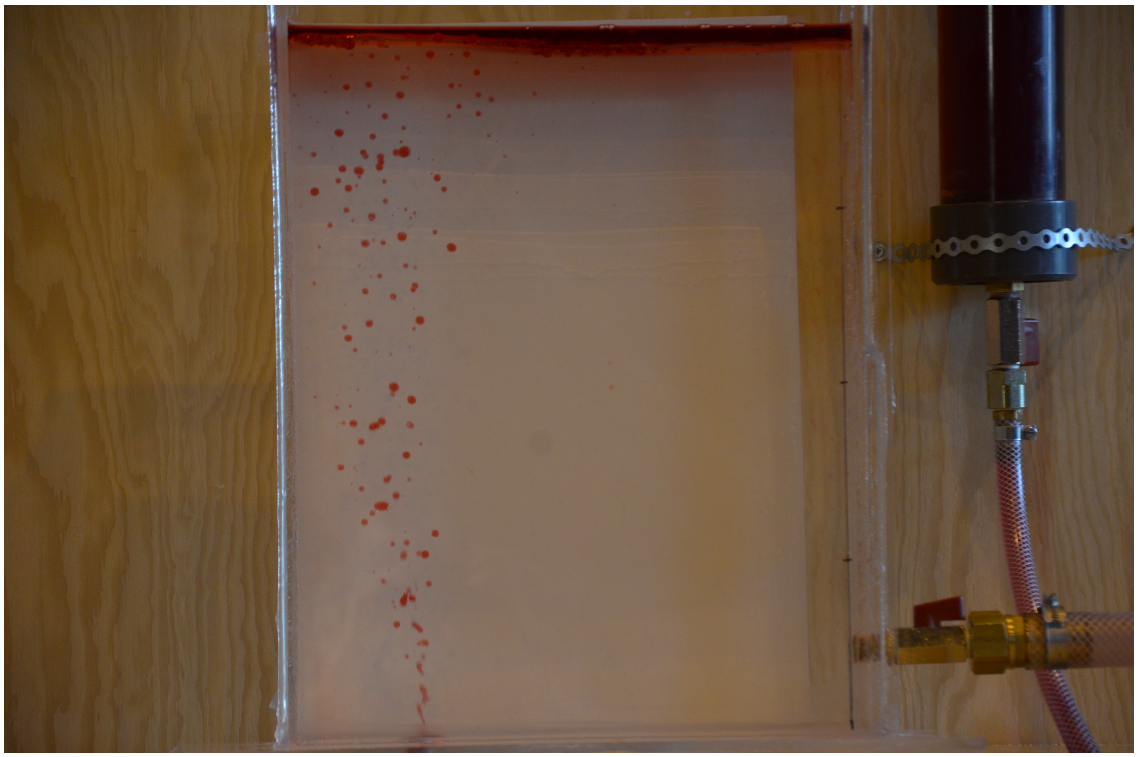

Figure A.6: Testing in tank 2 with a pressure drop of 1.0 bar across the valve and pump voltage 10.5 V

Figure A.7: Testing in tank 2 with a pressure drop of 0.5 bar across the valve and pump voltage 11.5 V

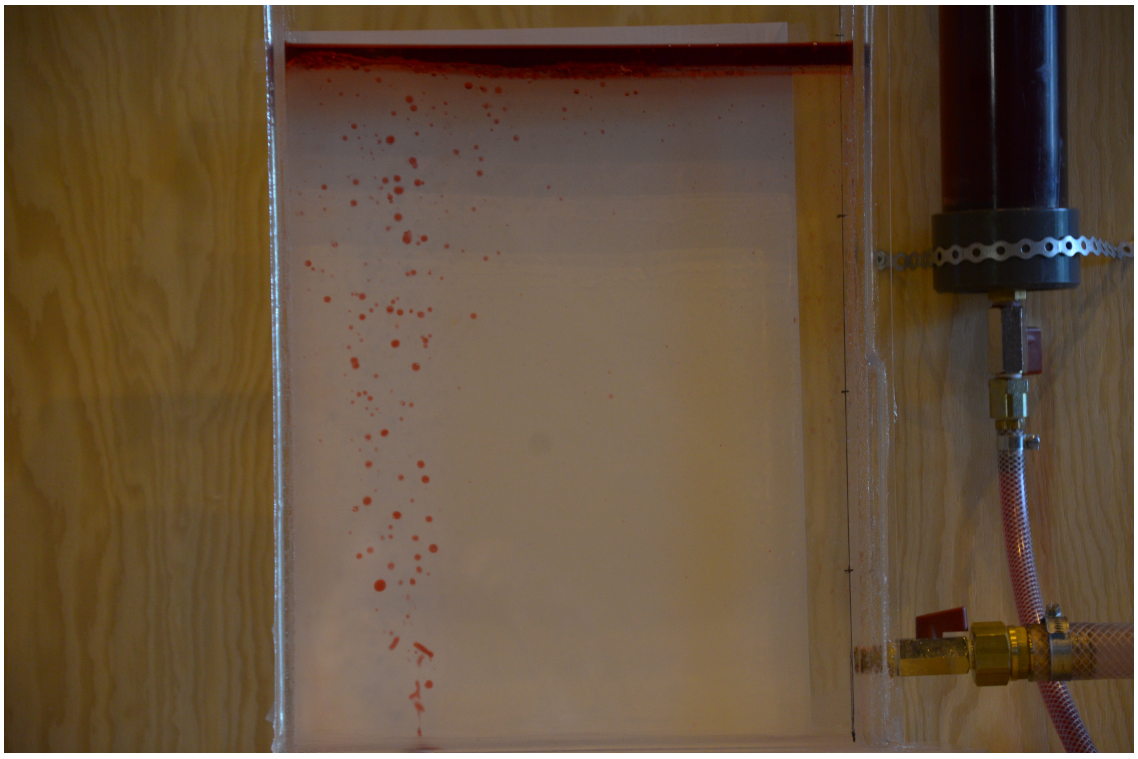

Figure A.8: Testing in tank 2 with a pressure drop of 1.0 bar across the valve and pump voltage 11.5 V

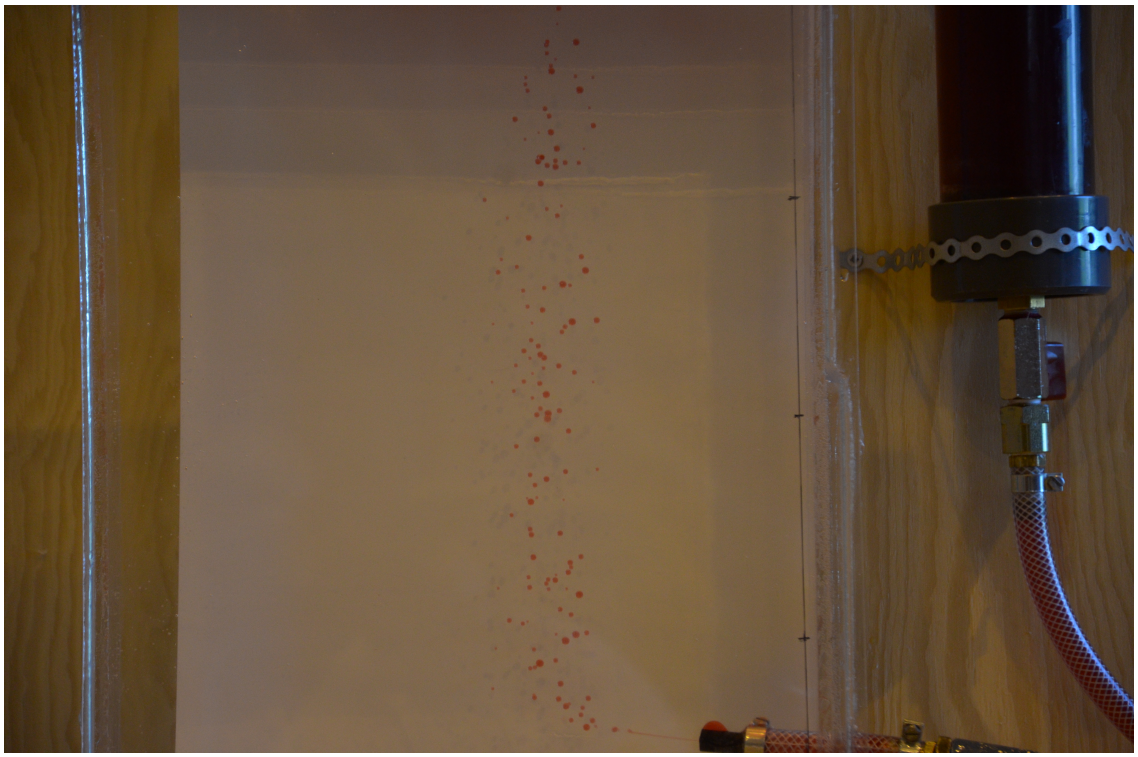

Figure A.9: Testing in tank 2 with a pressure drop of 0.6 bar across the nozzle

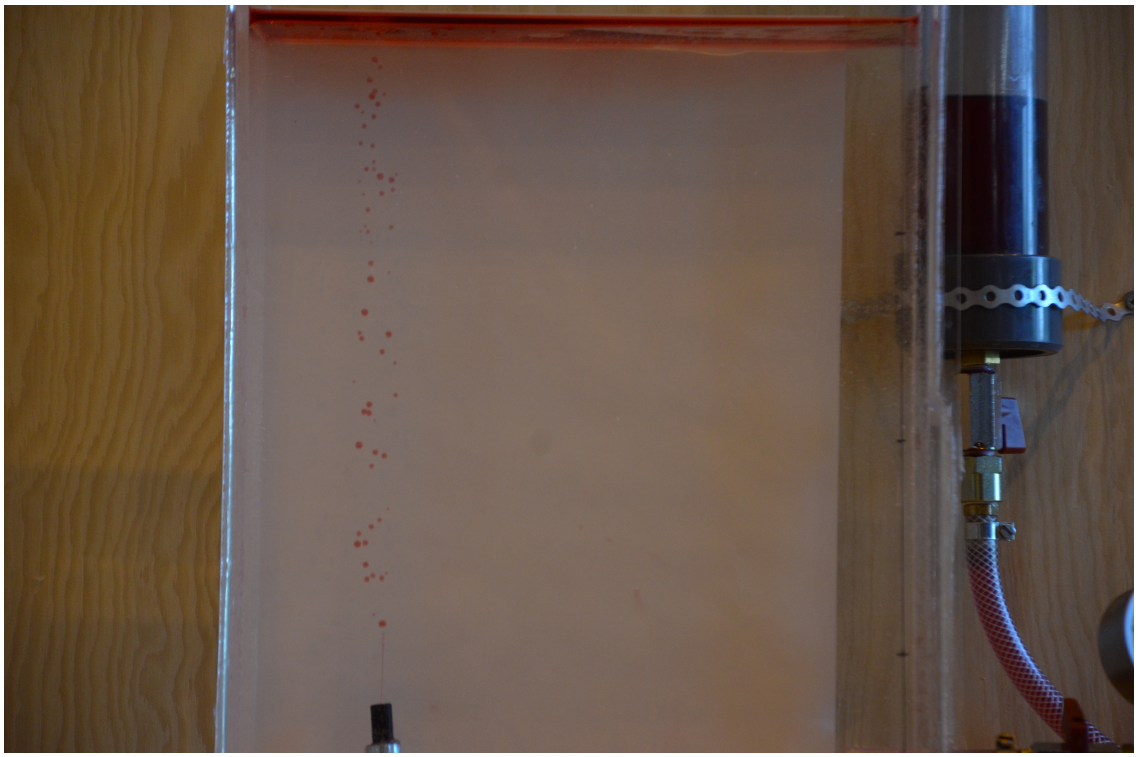

Figure A.10: Testing in tank 2 with a pressure drop of 0.6 bar across the nozzle

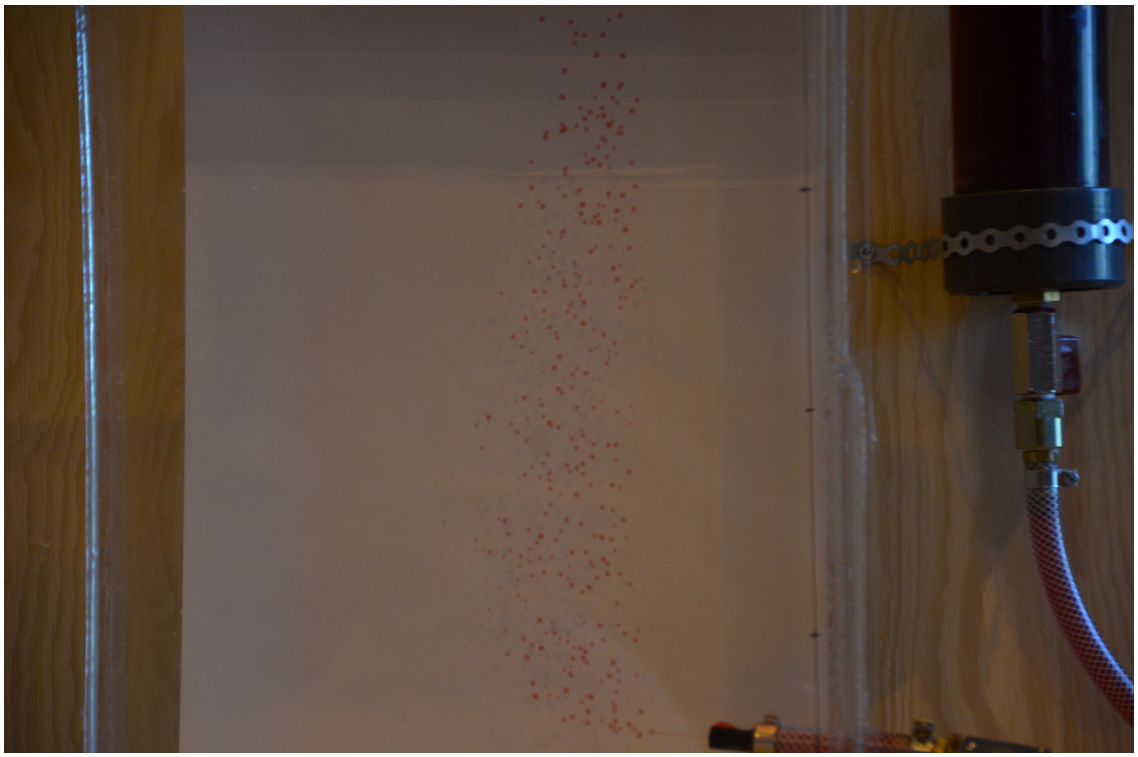

Figure A.11: Testing in tank 2 with a pressure drop of 0.8 bar across the nozzle

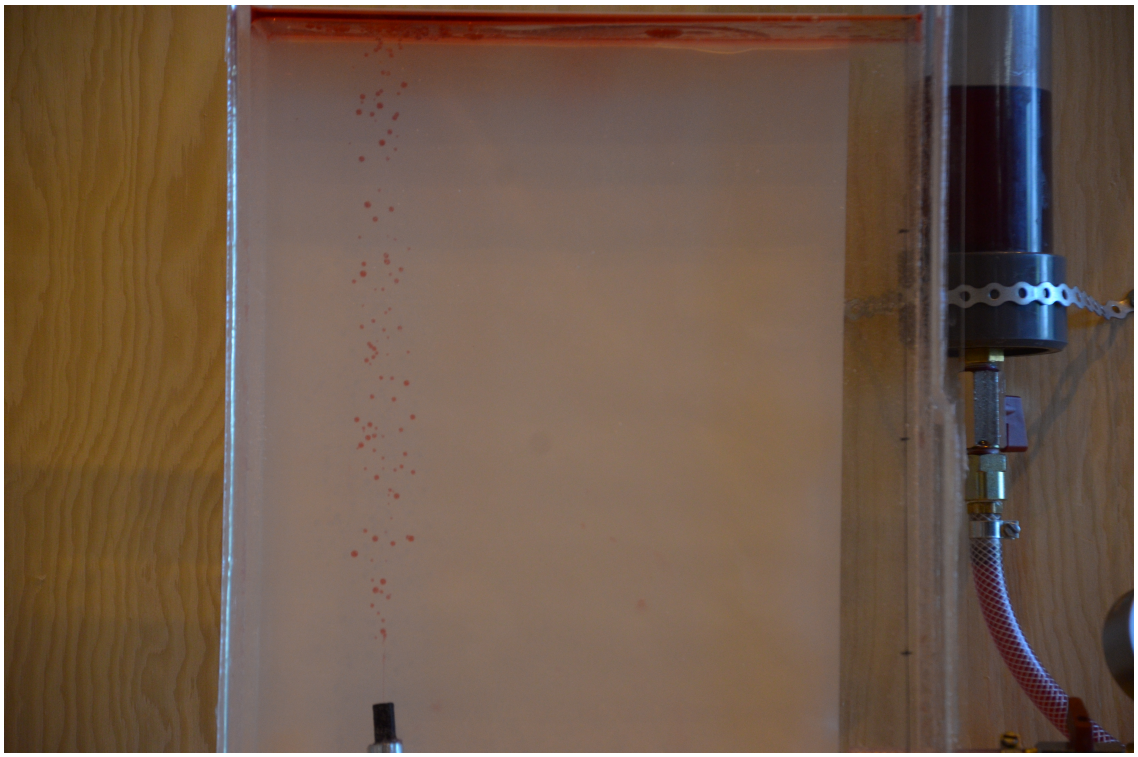

Figure A.12: Testing in tank 2 with a pressure drop of 0.8 bar across the nozzle

Figure A.13: Testing in tank 2 with a pressure drop of 1.0 bar across the nozzle

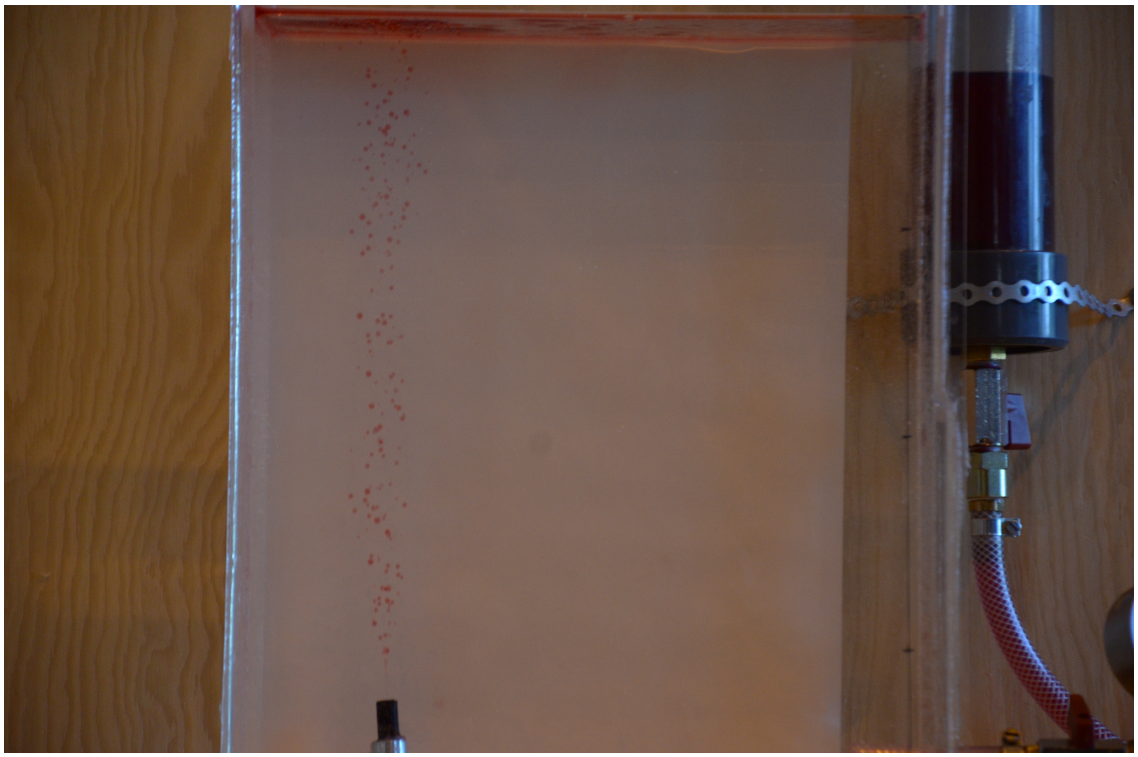

Figure A.14: Testing in tank 2 with a pressure drop of 1.0 bar across the nozzle

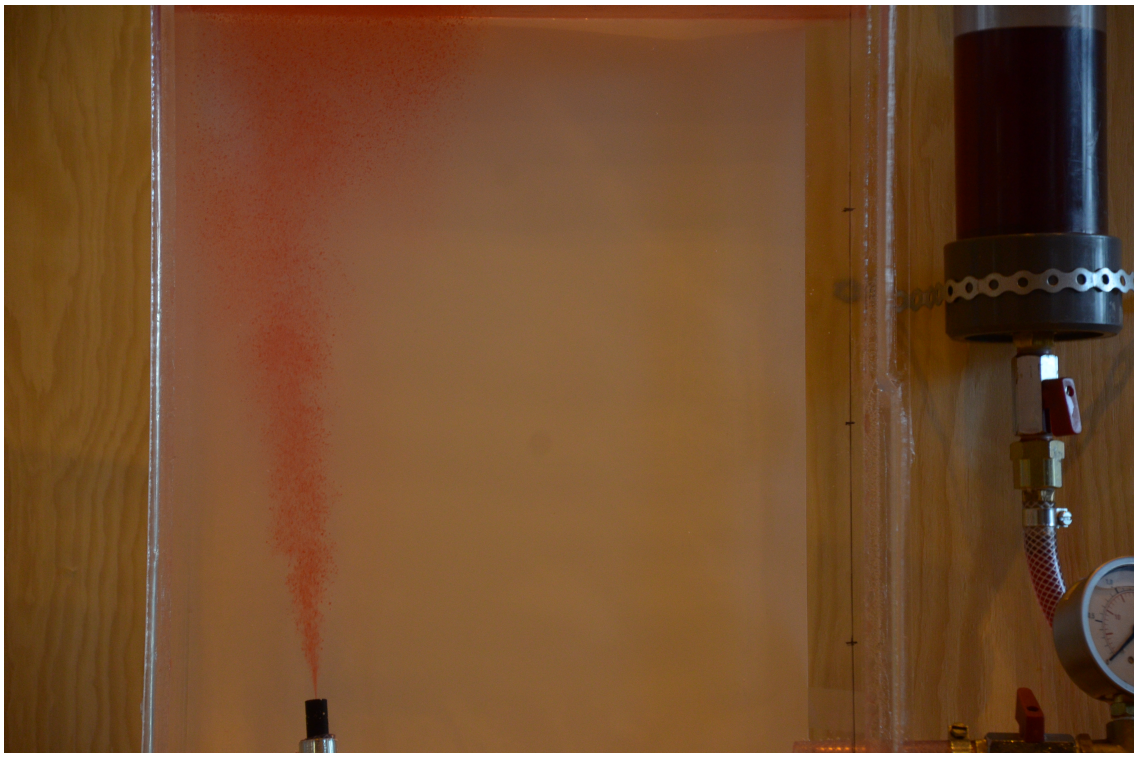

Figure A.15: Testing in tank 2 using paraffin and with a pressure drop of 0.2 bar across the nozzle

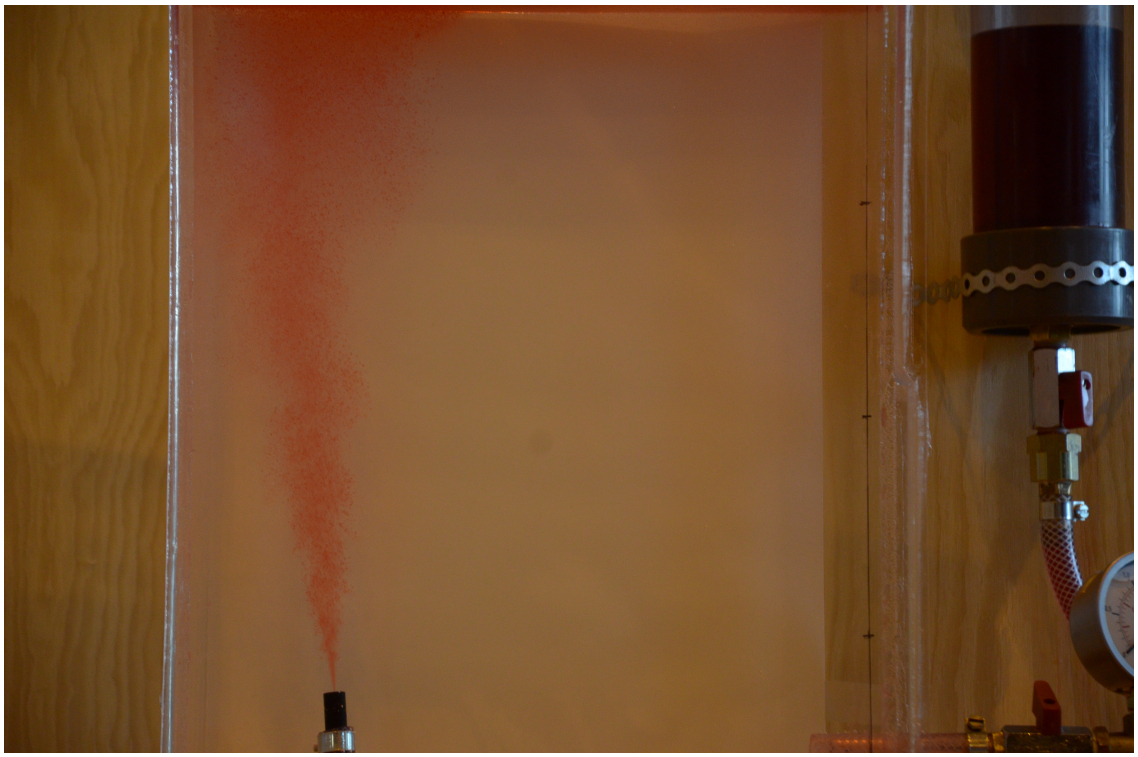

Figure A.16: Testing in tank 2 using paraffin and with a pressure drop of 0.3 bar across the nozzle

Figure A.17: Testing in tank 2 using air and with a pressure drop of 0.5 bar across the nozzle

Figure A.18: Testing in tank 2 using air and with a pressure drop across the nozzle just enough to give air flow